

# **A review of the Brasiliano magmatism in southern Espírito Santo, Brazil, with emphasis on post-collisional magmatism**

**Cristina P. De Campos**

Department of Geology - IGEO - CCMN - UFRJ - Ilha do Fundão, Cid. Universitária - Rio de Janeiro, R.J. - 21949-900, Brazil  
2 Dep. of Geology / Univ. of Munich / Germany. Theresienstr. 41/III M-80 333.  
*Email: campos@min.uni-muenchen.de*

**Júlio Cezar Mendes**

Department of Geology - IGEO - CCMN - UFRJ - Ilha do Fundão, Cid. Universitária - Rio de Janeiro, R.J. - 21949-900, Brazil

**Isabel P. Ludka**

Department of Geology - IGEO - CCMN - UFRJ - Ilha do Fundão, Cid. Universitária - Rio de Janeiro, R.J. - 21949-900, Brazil

**Silvia R. de Medeiros**

IG – Geosciences Inst./ Univ. of Brasília/ UnB – Asa Norte – CEP 70 910-900 – Brasília – D.F. / Brazil

**Jorge C. de Moura**

CNEN – Comissão Nacional de Energia Nuclear – \* CNPq – Conselho Nacional de Pesquisas

**Carin Wallfass**

Department of Geology - IGEO - CCMN - UFRJ - Ilha do Fundão, Cid. Universitária - Rio de Janeiro, R.J. - 21949-900, Brazil

Keywords: Neoproterozoic, continental collision, Brasiliano orogen, granites, enderbites, magma mingling

**Abstract:** Located at the Atlantic continental margin of Brazil, the Espírito Santo State links two Brasiliano-age fold belts: the northern Ribeira Belt and the southern Araçuaí Belt. In the central part of this region a deeply eroded crust is exposed, disclosing the roots of the Araçuaí-Ribeira Belt and the core of a continent-continent collision, which took place during Precambrian times. During the main collisional event (from W to E: 590 Ma to 575 Ma), considerable crustal thickening was generated from large to small scale isoclinal folding, refolding and the piling up of crustal segments and flakes along thrust faults. In this work we describe the major igneous events of the orogen, focusing particularly on the early and late post-collisional plutonism.

Metamorphism in the central zone of the orogeny reached high amphibolite to granulite facies at ~ 590 Ma and produced a high-grade metamorphic complex made up mostly of sillimanite + garnet ± cordierite ± biotite kinzigitic gneisses grading into hypersthene granulites, sillimanite quartzite and marbles. These rocks were intruded by syn-collisional tonalitic magmas at ~580 Ma associated with widespread crustal anatexis (anatexis I) and the coeval intrusion of minor amounts of basic to intermediate magmas.

This early high-grade metamorphism was followed by cooling and then reheating of the gneisses and granulites, which caused retrograde metamorphism, new partial melting (anatexis II) and the early post-collisional phase of enderbitic magmatism at around 560 Ma. The youngest magmatic phase, known as the late post-collisional magmatism, is characterized by sills, dykes and mostly bimodal complexly zoned plutons with extensive mingling between, and varying in composition from orthopyroxene-gabbro to granite. They intruded between 530 to 480 Ma with a peak at 500 Ma, and were associated with the third phase of anatexis (anatexis III). Metaluminous to peraluminous, high-K calc-alkaline, I-type granitoids of this late post-collisional phase progressively evolve into more markedly alkaline suites. While the early post-collisional sequences were probably generated by dehydration melting of a metasedimentary crust with small contributions from other sources, the late post-collisional association originated from contrasting sources: a) partial remelting from a mainly metaluminous continental crust, b) new dehydration melting from slightly peraluminous crustal portions, and c) important mafic contributions from an enriched mantle.



## Table of Contents

Introduction .....	5
Regional Geology .....	5
Main Magmatic Phases: A brief summary .....	7
Early post-collisional magmatism in the costeiro complex .....	8
Geochemistry: comparing G1, G2 and G3 .....	11
The late post-collisional magmatism .....	14
Geology of the plutons .....	14
Geochemistry and Geochronology of the Late Post-Collisional Magmatism .....	20
Conclusion .....	22
Acknowledgements .....	23
References .....	23
A. Field Trip .....	27
The coast near Vitória and Guarapari .....	28
Outcrop 1: Praia da Costa, in Vitória (UTM coordinates: 36630 – 775100) .....	28
Outcrop 2: Ubu Beach in Anchieta (UTM coordinates: 33550 – 769900) .....	28
Outcrop 3: Pau Grande Beach in Anchieta (UTM coordinates: 32500 – 769630) .....	28
Outcrop 4: Small quarry close to Iriri town (UTM coordinates: 332850 – 7769700) .....	28
Outcrop 5: Outcrops on the Enseada Azul Beach (UTM coordinates: 34150 – 770680) .....	28
The Guarapari coast and the cachoeiro de itapemirim region .....	29
Outcrop 6: Quarry north of Guarapari (UTM coordinates: 34750 – 771930) .....	29
Outcrop 7: Ponta do Pescador Outcrop (UTM coordinates: 34700 – 771500) .....	29
Outcrop 8: Perocão Beach (UTM coordinates: 34903 – 771750) .....	29
Outcrop 9: (UTM coordinates: 27540 – 769500) .....	30
G5 complex zoned plutons .....	30
Santa Angelica - A frozen-in magma mixing .....	30
Castelo Complex - A frozen-in contact .....	30
Pedra Azul - Mature Magmatism .....	32
B. Tables .....	34

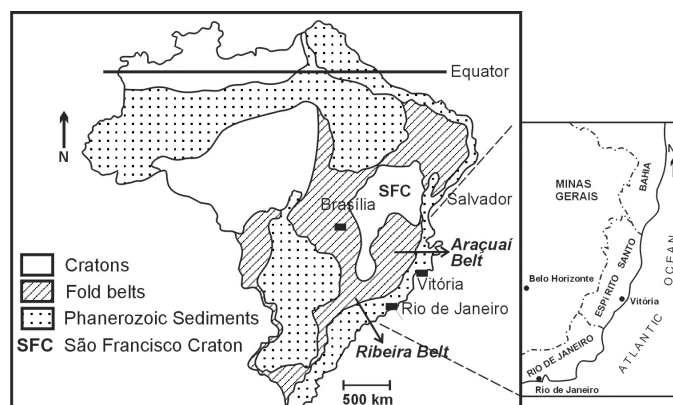
## Introduction

Around 600 million years ago sections from the older continent Rodinia collided in an extensive worldwide mountain building event known as the PanAfrican/Brasiliano orogen. Several branches from these orogenic terranes are nowadays exposed in Brazil, such as the Borborema, Tocantins and the Mantiqueira orogens [Brito Neves et al, 1999]. In this work we focus a segment of the Mantiqueira system: the region of Espírito Santo, north of Rio de Janeiro, which is well known for its prosperous dimension stone industry. Brasiliano-aged granites, gneisses, migmatites and marbles from this region are exported all over the world and make up nowadays around 47% of the total Brazilian stone industry.

During the last 25 years, after detailed geological mapping, geochemical and geochronological studies, a deeper understanding of its geological evolution has emerged. Most of the rocks cropping out in this region are of Brasiliano/ PanAfrican age and belong to the monocyclic Araçuaí-Ribeira Mobile Belt surrounding the São Francisco Craton ( Figure 1 ).

This paper reviews geological, geochemical and geochronological studies on Espírito Santo focusing on magmatic events. It starts with an overview of the regional geology followed by the chronology of tectonic events. In this way the first units to be outlined will be the high-grade gneisses (~580 Ma), which intruded short after the main collisional phase (~590 Ma). The paper then focus on the early post-collisional magmatic phase (575-560Ma) when enderbites are formed in the coastal region. After that, it covers the late post-collisional to post-orogenic phase (~530 to 480 Ma), which took place after a period of magmatic quiescence, when several bimodal plutonic complexes intrude the previous sequences. In the appendix, we present a field guide for the surroundings of the town of Guarapari, where early post-collisional enderbites crop out, and for the regions of Santa Angélica, Castelo and Pedra Azul plutons, where late post-collisional plutons crop out.

Figure 1. Location map modified after Almeida et al., 1973.

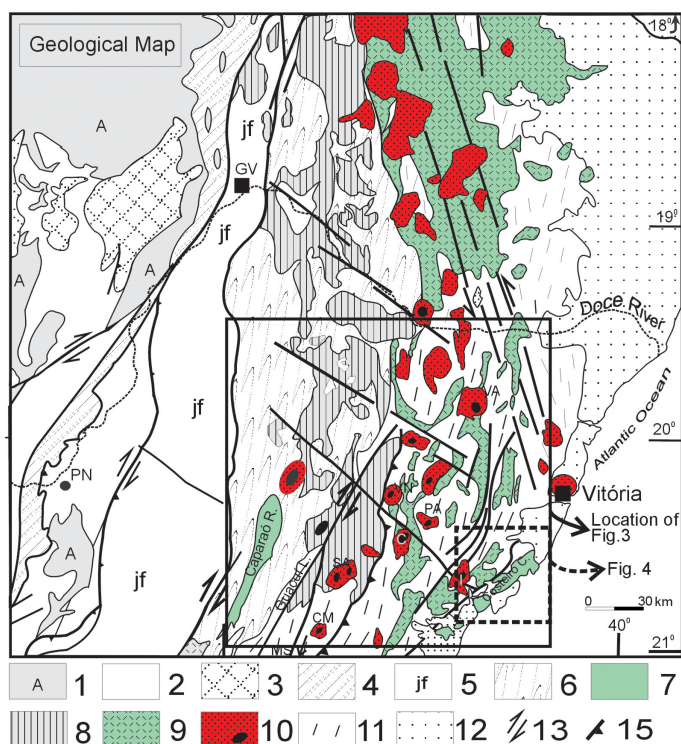


Location map modified after Almeida et al., 1973.

## Regional Geology

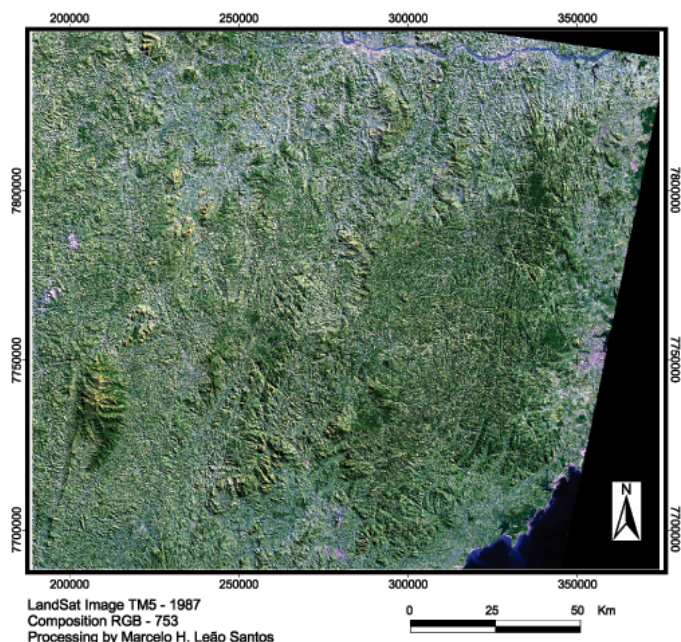
The Brazilian Atlantic coast, between southern Bahia and southern Espírito Santo States, consists of Neoproterozoic rocks from the Araçuaí Mobile Belt ( Figure 1 ) [Pedrosa Soares and Wiedemann-Leonardos, 2000; Pedrosa Soares et al., 2001], with predominant N-S structural trends. South of 21° S the Araçuaí Mobile Belt inflects from N-S to NE-SW known as the Ribeira Belt [Almeida et al., 1973; Heilbron et al., 2000; Trouw et al., 2000]. The regional geological map on Figure 2 shows the main units of this segment and the northernmost parts of this gentle inflection displayed on the satellite image of Figure 3. This crustal section is part of Western Gondwana and continues in Africa as the West-Congo belt. A complex collision between the São Francisco Craton, now in Brazil, and the Congo/Angolan Craton, now in Africa, drove the evolution of this belt.

**Figure 2. Geological map of the southern Araçuaí-Ribeira Belt**



Geological map of the southern Araçuaí-Ribeira Belt and cratonic surroundings, highlighting the Neoproterozoic units (modified from Pinto et al. 1998, Pedrosa Soares and Wiedemann-Leonardos, 2000; Wiedemann et al., 2002). 1 Achaeon meta-sediments; 2 TTG complexes, with greenstone belts remnants and metasedimentary units; 3 Paleoproterozoic Borrachudos granitoid Suite; 4 Salinas Formation metavolcanic-sedimentary unit (correlated to Dom Silvério Group); 5 Juiz de Fora Complex; 6 Rio Doce Group; 7 granulite facies domain of Paraíba do Sul Complex, Late Paleoproterozoic and Mesoproterozoic; 8 and 9 Late Neoproterozoic to Cambrian metagranitoid suites: 8 I-type G1 suite (predominantly tonalite- grading into granodiorite- and granite- gneisses with minor amounts of diorite-, amphibole-gneisses, amphibolite and metagabbro); 9 S-type G2 and G3; 10 Late Cambrian to Ordovician granitoid suites: I-type G5 (black dots represent the mafic cores of plutons); 11 high-amphibolite facies domain of Paraíba do Sul Complex; 12 Phanerozoic Covers; 13 Magnetometric anomalies of the studied plutons; 14 oblique to strike-slip faults or ductile shear zones; 15 thrust and detachment faults or ductile shear zones. Cities: GV, Governador Valadares; PN, Ponte Nova. References in text.

**Figure 3. Landsat image of the region**



Landsat image of the region showed in the geological map on Fig. 2.

The tectonic history of the Araçuaí-Ribeira belt is dominated by the amalgamation of a number of tectonic blocks from the closure of different segments of the Adamastor ocean (Pedrosa Soares et al., 2001; Brito Neves et al., 2000). The first record of subduction-related juvenile, intraoceanic, calc-alkaline volcano-plutonic arc was recognized in the southern region, in Rio de Janeiro State: the Rio Negro magmatic arc, at ~ 630 Ma. The accretion of this arc to the neighboring Transamazonian Juiz de Fora terrane (< 1700 Ma.) took place at ~ 600 Ma [Tupinambá et al., 2000]. Further north a well-defined gravimetric discontinuity, the Manhauçu discontinuity, in Minas Gerais State, marks the boundary between the Transamazonian Juiz de Fora terrane and the Araçuaí Mobile Belt [Wiedemann et al., 2002]. The main oceanic plate convergence took place along the entire belt between ~ 600 - 580 Ma, forming a new intracontinental plutonic arc with strong crustal contribution (G1 granitoids, see below; Geiger, 1993; Brito Neves et al., 2000).

The post-Transamazonian supracrustal rock pile in the Araçuaí-Ribeira belt is known as Paraíba do Sul Complex (units 7 and 11 on Figure 2 ). U-Pb SHRIMP determinations on detritic zircon from this unit yielded 207Pb/206Pb age peaks varying from 2104 Ma, 774 Ma up to 631.19 Ma (Noce et al., 2004) which have been interpreted as the

maximum and minimum source ages for the sediments. Rocks of this complex are subdivided into two units (Schobbenhaus et al., 1984): the Embú or Paraíba do Sul Complex *sensu strictu* (predominantly amphibolite facies - unit 11, in Figure 2) and the Costeiro Complex (predominantly granulite facies - unit 7). The Paraíba do Sul Complex consists mainly of a metasedimentary inhomogeneous package of partially migmatized banded gneisses, metamorphosed in the amphibolite to amphibolite-granulite facies transition. Metamorphic peak gave rise to the following paragenesis: garnet-biotite-plagioclase-microcline-quartz, garnet-cordierite-sillimanite-biotite-oligoclase/andesine-microcline, hypersthene-augite-andesine/labradorite and garnet-quartz-hornblende-biotite gneisses, biotite-garnet-cordierite-sillimanite-graphite gneiss, dolomitic and calcitic marbles and sillimanite-quartzite (Leonardos & Fyfe, 1974; Sluitner & Weber-Diefenbach, 1987; Féboli, 1993).

The Paraíba do Sul and Costeiro Complexes preserve rocks formed in two marine environments: 1) a proximal marine environment, probably a shallow shelf which received terrigenous siliciclastic material to produce common sandy rocks (graywacke gneisses and sillimanite-quartzite) interlayered with thick carbonatic layers; 2) a distal pelite-rich marine environment with minor carbonatic intercalations. The presence of graphite and high H<sub>2</sub>S-contents in the marbles point towards reducing conditions during the sedimentation process and confirm a shallow shelf marine environment (Geiger, 1993). Distal pelites gave rise to extensive kinzigitic gneisses with thin calc-silicate lenses (Ubu series). Scarce leptinite (a garnet-rich, biotite-poor leucocratic gneiss) and orthoamphibolite interlayered with kinzigitic gneiss indicate that alumina-rich shales accumulated in deeper marine environments with restricted mafic volcanic contribution (Pedrosa-Soares & Wiedemann-Leonardos 2000). Geochemical data from biotite- and biotite-amphibole-gneiss confirm that pelitic sediments and subgraywacke are the most probable protoliths (Geiger, 1993). Small igneous intrusions, consisting of metamorphosed gabbro, pyroxenite, diorite and biotite-andesine granitoids are also found in these terrains.

In summary, the Paraíba do Sul and Costeiro Complexes represent sedimentary marine sequences of Neoproterozoic age intruded during sedimentation (> 600 Ma) by small volumes of mostly basic magma and metamorphosed during the main collisional phase (from 600 to 575 Ma) to amphibolite/granulite facies. In the central part of

Espírito Santo the roots of the Brasiliano Belt are exposed, revealing NE-trending, granulitic sequences, including kinzigites (coarse-grained sillimanite-cordierite-bearing granulites of the Paraíba do Sul Complex) interfingering with granitic-granodioritic gneisses (Delgado & Marques, 1993; Cunningham et al., 1998). The main collisional stage of the Brasiliano Araçuaí-Ribeira with the West-Congo Orogen, in this region, took place diachronously from ~600 Ma in the surroundings of the Caparaó Ridge, in the west (Sm-Nd whole-rock from granulites of the Caparaó, Fischel, 1998), to ~560 Ma, in the easternmost coastal region (U-Pb on zircons from granulites of the coastal region, Söllner et al., 2000). This compressive deformation episode caused crustal shortening of at least ~30 to 40% (Fritzer, 1991) and produced west-verging, moderately- to steeply-dipping thrusts (Pedrosa Soares et al., 2001). This process was accompanied by the development of metamorphic or migmatitic layering and tight to isoclinal folds (D1), refolded to form long-wavelength folds with upright to slightly west-verging axial planes and amplitudes up to 10 km (D2) such as the Caparaó ridge, a NE-SW-trending structure (the large hook-shaped mountain on the SE corner of Figure 3; Lammerer, 1987; Fritzer, 1991). Such folding is associated with contemporaneous stretching parallel to the horizontal plunging fold axes, indicating a prominent transpressive regime. At a late stage dextral, high-angle, oblique- to strike-slip shear zones truncated the previous folding. The Guaçuí lineament, east of the Caparaó ridge, is one of the most notable shear zones in this region (Figure 2).

This thick continental crust underwent different ultra-metamorphic conditions in different regions of the belt. While the westernmost granulites from the Caparaó Ridge crystallized at  $586 \pm 2$  Ma, under P-T conditions exceeding 10 kb and 800°C (Seidensticker, 1990), along the Coastal region the formation of enderbite granulites, under lower P-T conditions, was around  $558 \pm 2$  Ma (Söllner et al., 2000).

## Main Magmatic Phases: A brief summary

Regional geochronological and geological criteria has led to the subdivision of orogenic magmatism in the Araçuaí-Ribeira Belt into G1, G2, G3, G4 and G5 (Wiedemann et al., 1986; Wiedemann, 1993; Ludka et al., 1998; Pedrosa-Soares et al., 1999, 2001; Ludka & Wiedemann, 2000; Medeiros et al., 2000, 2001, 2003; Mendes et al. 1997,

1999, Wiedemann et al., 2002). The G1 and G2 suites (~580 Ma) are syn-collisional phases but have different proportions of source components. The G3 granitoids are less voluminous and resulted from the remelting of the previous ones, in an early post-collisional stage (~560-535 Ma). The G4 suite is restricted to the northwestern part of the belt and is not considered in this study any further. The G5 suite (~500 Ma) records the youngest post-collisional magmatic episode in the area.

The G1 suite consists of tectonically foliated tonalite, granodiorite and minor granite and diorite (unit 8 in Figure 2), usually showing deformed K-feldspar augen megacrysts in a foliated biotite-rich matrix. Mafic to intermediate microgranular enclaves up to gabbroic compositions, are commonly found stretched along the gneissic foliation (Lammerer, 1987; Fritzer, 1991; Geiger, 1993; Wiedemann et al., 1997, 2002). These granitoids are considered syn-collisional as they show the same deformation as the enclosing gneisses. U-Pb zircon ages (Söllner et al., 1991) constrain crystallization of G1 granitoids, in Espírito Santo, to between 586 and 575 Ma. Part of the syn-collisional G1 magmas crystallized under dry conditions and high CO<sub>2</sub>-pressures (Fritzer, 1991; Wiedemann et al., 1997; Mendes et al., 1997) originating magmatic charnockitoids with noritic cores. As an example the hypersthene-bearing orthogneiss from the Serra do Valentim, north of the Caparaó ridge, was formed under temperatures around 800 °C and pressures of 8 to 9 kb (Fritzer, 1991; Seidensticker & Wiedemann, 1992).

Geochemical data from several G1 plutons point towards calc-alkaline, metaluminous to fairly peraluminous magmas, formed in a volcanic arc setting (Geiger, 1993; Campos-Neto & Figueiredo, 1995; Wiedemann et al., 1997; Pedrosa-Soares et al., 1999). Pre-collisional calc-alkaline granitoids, such as the Rio Negro granitoids described further south (Heilbron et al., 2000) have not yet been recognized in this area but zircons of similar age (631 ± 19 Ma) are found in the Paraíba do Sul metasedimentary rocks (Noce et al., 2004). Based on geochemical and structural studies of G1 granitoids and enclosing rocks, Geiger (1993) proposed a geodynamic model for the area with a two-stage island arc evolution and two plate collisions. G1 granitoids have been then interpreted to represent the roots of a second subduction related magmatic arc, which intruded and crystallized short after the peak of metamorphic conditions. Further detailed studies are necessary in order to separate the different G1 granitoids along the entire mobile belt.

G2 is another set of intrusions, locally with gradational contacts with the Paraíba do Sul complexes, which crops out in this region (unit 9 in Figure 2). It consists mainly of batholithic bodies of tectonically foliated, S-type, subalkaline to calc-alkaline, mostly peraluminous garnet-biotite granites (Pedrosa Soares & Wiedemann-Leonardos, 2000). Ghost migmatitic structures and ubiquitous rafts of migmatites and paragneisses indicate a predominant autochthonous to para-autochthonous nature. A widespread process of in situ migmatization of the metasedimentary pile originated a "sea" of diatexites and foliated granites. G2 makes up the anatectic core of the Araçuaí-West-Congo orogen.

Around 560 Ma, after significant cooling, a new reheating of the gneissic/granulitic crust took place and resulted in retrograde metamorphism, under high-amphibolite/granulite conditions with restricted partial melting which generated the G3 suite (anatexis II). The retrograde metamorphism is well illustrated by the replacement of sillimanite by cordierite and of pyroxene by biotite (Sluitner, 1989; Kühn et al., 2004) and the development of symplectitic and coronitic textures in granulitic/charnockitic rocks (Wiedemann et al., 1997). Although very similar to the G2 granitoids, the G3 suite is clearly younger and non-foliated, save when it inherits ghost foliation from the source rocks.

At the end of the orogenic cycle, around 535-480 Ma, discordant G5 plutons intrude the area and caused a new phase of anatexis (anatexis III). During the last 25 to 30 years, this voluminous plutonism and its enclosing sequences were the focus of several geological, geochemical and geochronological studies by our group and collaborators.

The next section details the syn-collisional G2 and the late-collisional G3 suites (Wiedemann et al., 1986; Wiedemann, 1993; Ludka et al., 1998; Pedrosa-Soares et al., 1999, Ludka & Wiedemann, 2000; Medeiros et al., 2000, 2001, 2003; Mendes et al. 1997; 1999). This is then followed by a section describing examples of the late post-collisional G5 suite.

## Early post-collisional magmatism in the costeiro complex

The Costeiro Complex of southern Espírito Santo (Figs 2 and 4) is comprised of stromatic garnet-cordierite-sillimanite kinzigitic gneiss frequently interlayered with calc-silicate granulite (Ubu series) and less frequent leptinite (garnet-feldspar granulitic gneiss). Local changes in the original composition of the sedimentary pile account for

gradual changes into more metaluminous layers of biotite-amphibole-garnet gneiss. This predominantly metasedimentary rock pile is partially melted and intruded by metaigneous high-amphibolite to granulitic gneisses, with prevailing hypersthene granodioritic to tonalitic compositions (G2 enderbites) and restricted quartz-monzonitic to granitic compositions (G2 charno-enderbites), locally with garnet. Contacts are mostly gradational but occasionally sharp, suggesting a tectonic control. The G2 enderbites form then green-colored discontinuous patches with diffuse boundaries within G2 grey amphibolitic gneisses (Figure 5 and 6) and kinzigite of the Costeiro Complex (Figure 4). The strongly foliated and variably migmatitic green to grey G2 gneisses are then cross cut by younger non-deformed granitic and pegmatite veins [Sluitner and Weber-Diefenbach, 1989; Féboli, 1993; Wiedemann et al., 1997; Teixeira, 1998].

Figure 4. Geological map of the Costeiro Complex

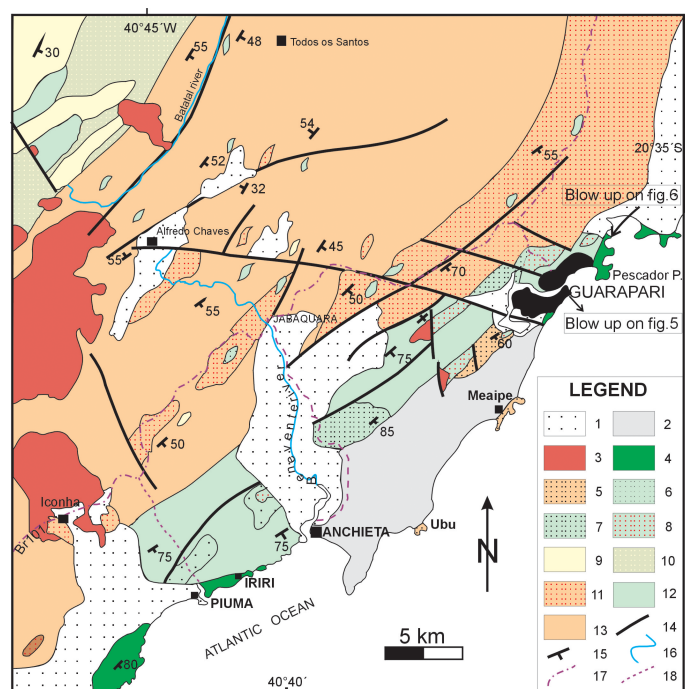


Fig. 4

Geological map of the Costeiro Complex (modified from Sluitner & Weber-Diefenbach, 1989). Legend: 1 Alluvial and Quaternary deposits; 2 Barreiras Formation (Tertiary); 3 Cambro-Ordovician intrusive rocks; 4 Iri-ri-series, alternation of enderbitic gneisses with porphyroblastic feldspar-gneisses and calc-silicates; 5 migmatitic garnet-cordierite-gneisses; 6 amphibolitic gneiss in alternation with granulites (predominantly enderbitic); 7 same as 6, mostly migmatitic; 8 garnet-bearing granulites (predominantly enderbitic); 9 sillimanite-quartzite; 10

alternation of quartzite and feldspar-gneisses; 11 garnet-biotite gneisses, locally migmatitic; 12 amphibolitic gneisses; 13 sillimanite-garnet-cordierite-gneisses (kinzigite); 14 lineaments (faults and shear zones); 15 foliation attitude; 16 rivers; 17 main roads; 18 secondary roads.

Figure 5. Detailed map from the Siribeira region

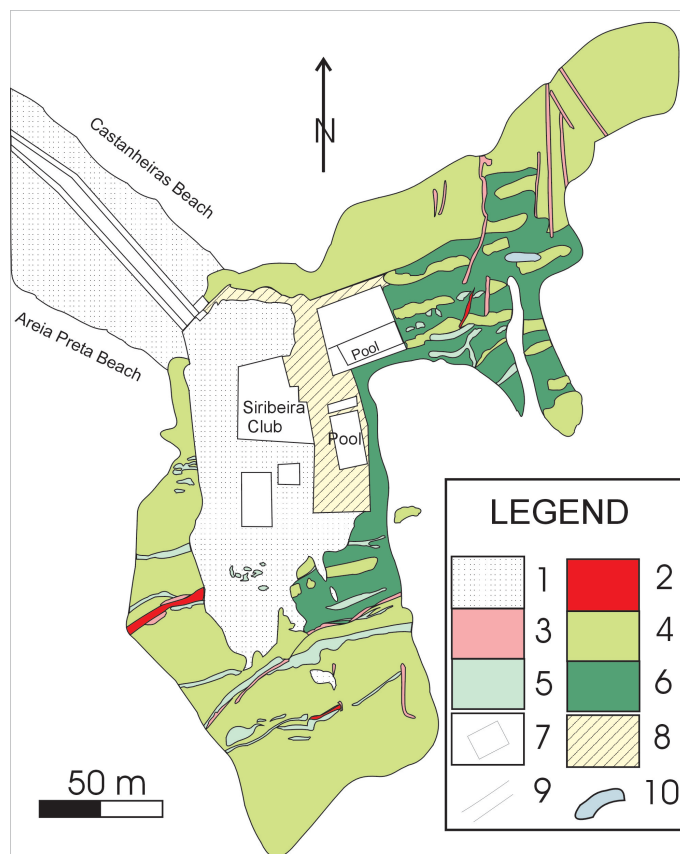


Fig. 5

Detailed map from the Siribeira region, southeast of Guarapari (modified after Teixeira, 1998). Legend: 1 quaternary deposits; 2 granitic veins; 3 pegmatite; 4 amphibolite-biotite-gneiss grading locally into enderbite; 5 leptinite; 6 domains dominated by enderbite; 7 house; 8 garden; 9 road; 10 water. Structural symbols as in Fig. 6.

**Figure 6. Gradational contact between amphibolite-biotite-gneiss and enderbite in the Siribeira region**

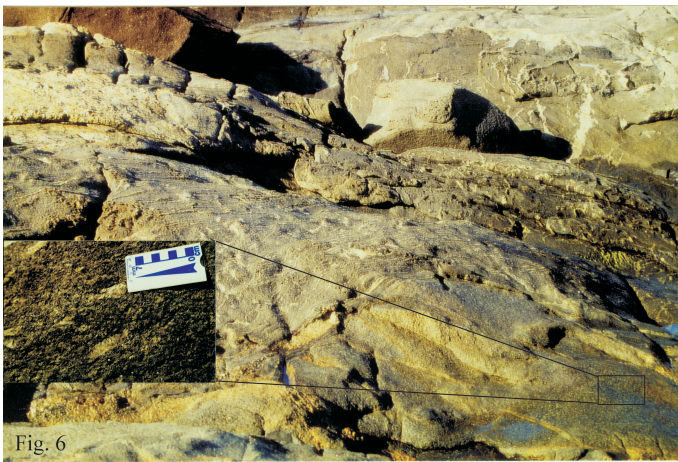


Fig. 6

Gradational contact between amphibolite-biotite-gneiss and enderbite in the Siribeira region. Geological map in Fig. 5. Note greenish color on the first plane of the photograph contrasting with grayish hues at the back. Blow up of a typical enderbite.

The region around the Perocão Beach, north of Guarapari town, ( Figure 7 ; see appendix 1 Field Guide) depicts, in a smaller scale, part of the complexity of the geology in the area. The predominant lithology consists of a foliated G2 metagranitoid (augen amphibolitic gneiss;  $575 \pm 12$  Ma U-Pb in zircons from Söllner et al., 1989) in contact with less foliated G3 enderbites. The age for G2 intrusive rocks corresponds to the first dehydration partial melting of the metasedimentary pile in the coastal region (anatexis I) and to the coeval intrusion of smaller amounts of less evolved, mafic melts. Remnants from the metasedimentary pile, consisting of kinzigite and calc-silicate rocks, crop out less than one kilometre southwards, along the Pescador Peninsula ( Figure 8 ). Around  $558 \pm 2$  Ma, a second dehydration melting episode culminated in the production of massive enderbitic domains trending along N-S directions, but partially preserving an older NE-SW foliation. This defines the G3 suite that resulted from the remelting of G2, anatexis II ( Figure 7 ). Pegmatite and granitic veins in this Outcrop cross-cut all the other lithologies and are the result of a third anatectic episode in the region around 500 Ma, anatexis III (Wiedemann et al., 2002). This last episode seems to be related to an extensional phase which originated NE-SW to N-S striking dykes and shear zones.

**Figure 7. Detailed map from the Perocão region, northwest of Guarapari**

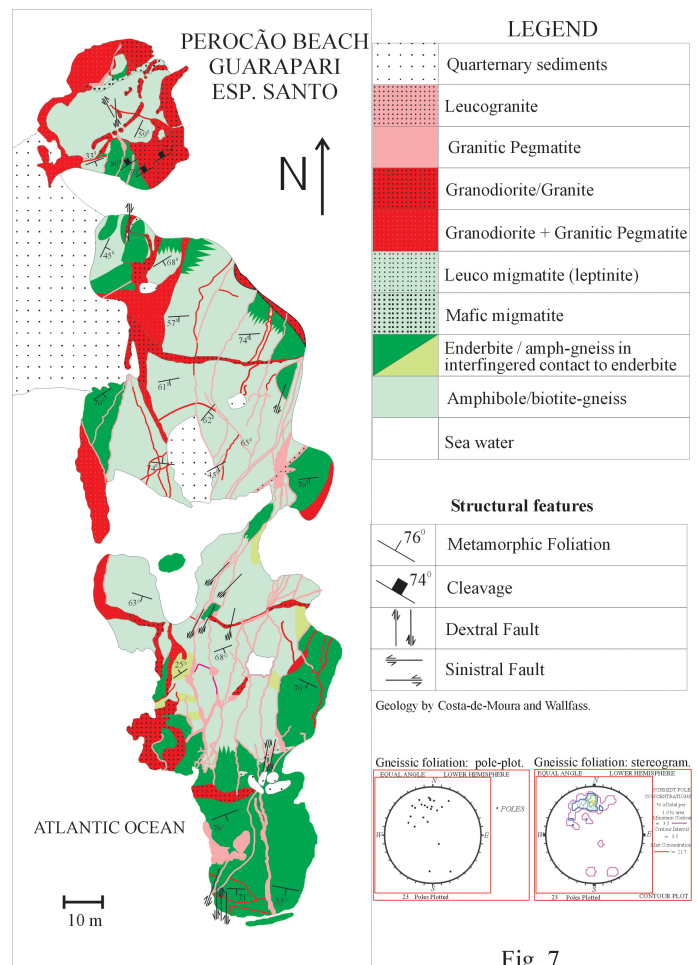


Fig. 7

Detailed map from the Perocão region, northwest of Guarapari. The interfingering pattern between enderbite and amphibolite-biotite-gneiss represents the gradational and irregular contacts between the two.

**Figure 8. Dehydration melting of the sillimanite-garnet-cordierite gneiss**



Fig.8

Dehydration melting of the sillimanite-garnet-cordierite gneiss (kinzigite) from the Pescador Beach, Guarapari. Garnet-bearing melts give rise to a stromatic fabric.

**Figure 9. R1-R2-multicationic diagram**

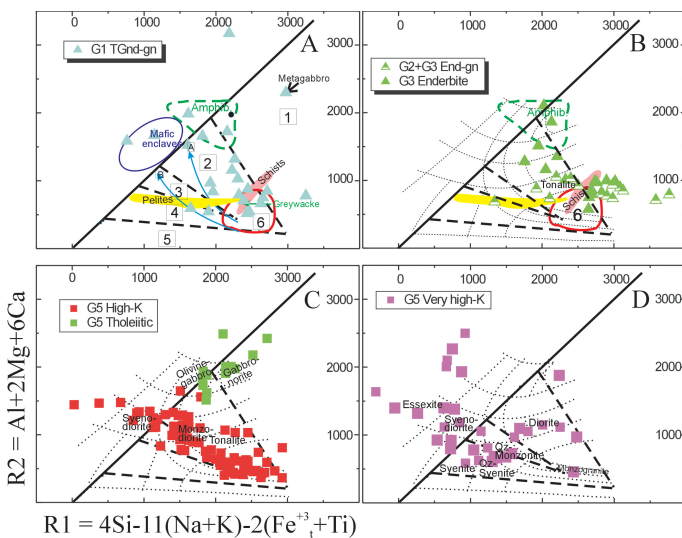


Fig. 9A,B,C,D

R1-R2-multicationic diagram (petrographic divisions after de la Roche et al., 1980); 1 mantle plagiogranite; 2 destructive active plate margin (pre-plate collision); 3 Caledonian permitted plutons (late orogenic); 4 sub-alkaline plutons (late orogenic); 5 alkaline / peralkaline magmatism (post-orogenic); 6 anatectic magmatism (syn-orogenic) (from Batchelor and Bowden, 1985). A: G1 tonalite to granodiorite gneisses (data from Geiger, 1993); mafic enclaves, amphibolites (abbreviated as amphib. in figure), Vectors from field 6 towards A and B indicate the change in melt composition under progressive equilibrium partial melting of rocks of monzodioritic (A) and monzonitic (B) bulk compositions; partial melting vectors (towards A and B) and metasedimentary

sources (greywacke, pelites, schists and field 6 from Batchelor and Bowden, 1985). B: G2 and G3 enderbites and enderbite-gneisses (data from Sluiter, 1987). C: G5 high-K [Santa Angélica and Castelo data from Horn, 1987; Iconha data from Offman, 1990; Pedra Azul data from Platzer, 1997; G5 tholeiitic suite (Jacutinga) from Ludka, 1997]. D: G5 very high-K suite (Mimoso do Sul data from Ludka, 1991; Venda Nova data from Horn, 1987). Individual plutons are not discriminated on this diagram. Discussion in text.

**Geochemistry: comparing G1, G2 and G3**

In order to evaluate the suggestion of a dominant sedimentary source for the generation of this early magmatic suites, geochemical data from G1, G2 and G3 suites from Sluiter, 1989, Offman, 1990 and Geiger, 1993 have been plotted on the multicationic diagram from de la Roche et al. (1980) and Batchelor & Bowden (1985) ( Figure 9a,b ). All these suites fall mainly in the second discrimination field, which accounts for an origin under predominantly destructive plate conditions. G1, with its mafic enclaves and metabasic intrusions plots towards field 1 (for mantle derivatives). G2 samples by contrast are dispersed at the prolongation of pelites and greywacke fields, corroborating the significant role of a sedimentary source in their origin inferred from field relationships. When compared with G1, most G2 samples plot in the same tectonic field 2, however, as an expanded group regarding the R1-axis towards field 1 and confirming the strong metasedimentary component. G3 compositions are restricted to the neighbourhood of field 6, for crustal melts, reinforcing field observations suggesting an origin from the partial remelting from G2. While G1 consists mostly of metaluminous tonalitic and granodioritic compositions, significant contribution of sediments in G2 and G3 drives their composition towards peraluminous granitic melts ( Figure 10a ). Nevertheless the presence of less evolved melts in the G2 suite in comparison to G3 suggests additional sources in the origin of G2.

Figure 10. A/CNK vs. A/NK

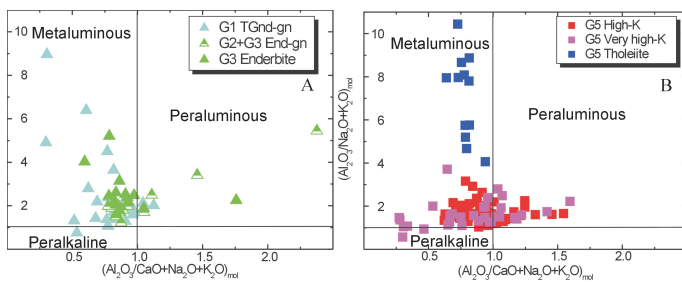


Fig.10A,B

A/CNK vs. A/NK (alumina saturation diagram from Shand, 1943). A: G1 tonalite to granodiorite gneisses (data from Geiger, 1993); G2 and G3 enderbites and enderbitic-gneisses. B: G5 high-K suite. Data sources as in Fig. 9. Discussion in text.

The metaigneous assemblage corresponding to suites G2 and G3 in the Costeiro Complex consists of continuous compositions from granodiorite to quartz-monzonite (Sluitner, 1989) with relatively uniform values of K<sub>2</sub>O (Figure 11a), Rb and Sr. The K<sub>2</sub>O-contents of the intermediate rocks are moderate to high. For the acidic rocks, like enderbite (hypersthene tonalite) and charnockite (hypersthene granite) anomalously high-K values could be the result of accumulation of K-feldspars through differentiation and/or tectonic processes, rather than represent a shoshonitic component in this magmatism.

Figure 11. SiO<sub>2</sub> x K<sub>2</sub>O diagram

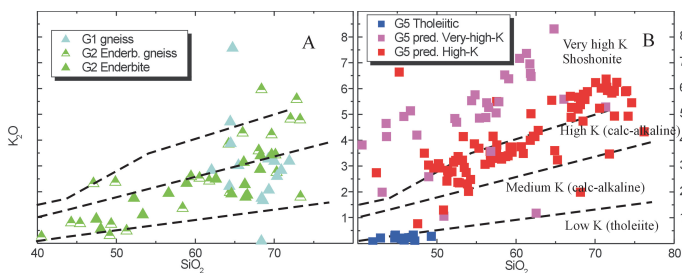


Fig.11A,B

SiO<sub>2</sub> x K<sub>2</sub>O diagram. A: G1 tonalite to granodiorite gneisses; G2 and G3 enderbites and enderbitic-gneisses. B: Fields from Le Maitre, 1989; G5 high-K and very high-K suite. Data sources as in Fig. 9. Discussion in text.

Ba- and Sr- contents in G1, G2 and G3 suites are high (typically 1000 ppm Ba for G2 and G3 and slightly less for G1; Figure 12a), even when compared to other igneous sequences of Pan-African ages (Rajesh, 2004; Asrat et al,

2004). G1 rocks are considerably richer in Sr than G2 and G3, particularly at high Ba contents. Chondrite normalized REE-diagrams are particularly useful for comparison between suites and their possible sources. Fractionated REE-patterns (La/Yb < 16) with moderate total values and very similar REE-patterns for samples from different but adjacent layers of enderbites (G2) and amphibolitic gneisses (G2) point towards similar sources.

Figure 12. Log Ba vs Sr diagram

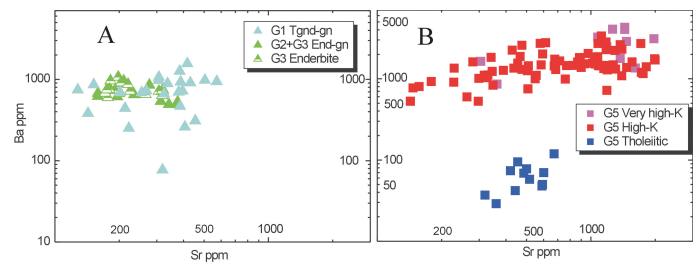


Fig.12A,B

Log Ba vs Sr diagram. A: G1 tonalite to granodiorite gneisses; G2 and G3 enderbites and enderbitic-gneisses. B: Fields from Le Maitre, 1989; G5 high-K and very high-K suite. Data sources as in Fig. 9. Discussion in text.

Figure 13a shows REE patterns from the most basic portions of the G1 suite: amphibolite to amphibolite-gneisses and metagabbros. With the exception of one metagabbro sample, showing lower total REE values, therefore a more depleted behaviour, all other metabasites depict a rather flat pattern with slight enrichments of light REE and about 10 times the chondrite amount for heavy REE. The metadiorite sample of G1 (Figure 13b) is very similar to the enriched metagabbroic ones, with no Eu-anomaly. The granodiorite and tonalitic to granitic gneisses, on the other hand, depict clear enrichment in light REE-patterns, with increasing negative Eu-anomalies for increasing differentiation. This could be explained through partial melting of a rock where feldspar is retained in the source. G2 and G3 suites show similar REE-patterns, which may be a further support for their consanguinity (Fig 13c,e). REE-patterns are similar to those of metasedimentary gneisses and kinzigite (Figure 13d), which suggests its involvement in the origin of G2 and G3 suites.

Figure 13. Rare Earth Elements abundances normalized to chondrite

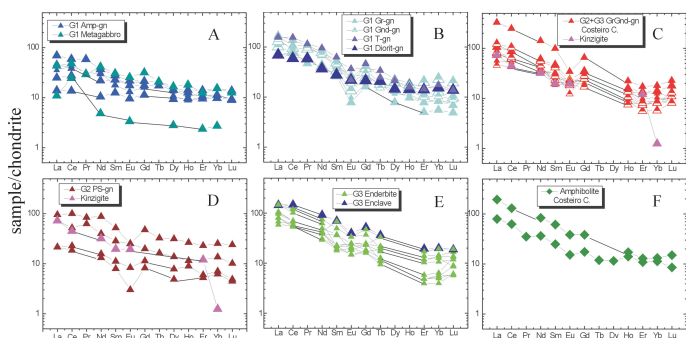


Fig.13A,B,C,D,E,F

Rare Earth Elements abundances normalized to chondrite (after McDonough and Sun, 1995) plotted against REE atomic numbers. A: G1 amphibole-gneisses and metagabbros B: G1 gneisses of granite, granodiorite, tonalite- and dioritic composition (from Geiger, 1993). C: G2 and G3 enderbite-gneisses; kinzigite (from Geiger, 1993). D: G2 garnet-gneisses and kinzigite (from Geiger, 1993). E: G3 enderbites and associated enclave (from Sluitner, 1987). F: Amphibolite from Costeiro Complex (from Sluitner, 1987). Discussion in text.

Similarities between preliminary Sm/Nd, U/Pb and Rb/Sr isotopic data, in minerals and whole rock, further suggests a common affiliation between amphibolitic, enderbite and kinzigitic gneisses ( Table 1 and Figure 14 ). Very high Sr87/Sr86 ratios and very negative Nd values are evidence of a predominant sedimentary origin for the magmatic suites. The side-by-side formation of enderbite and amphibolitic rocks was probably dependent on changes in the CO<sub>2</sub>/H<sub>2</sub>O pressure conditions. This process should be studied, in more detail, in order to decipher the precise formation mechanism for hypersthene-bearing rocks during the Neoproterozoic.

Figure 14. <sup>143</sup>Nd/<sup>144</sup>Nd vs. <sup>87</sup>Sr/<sup>86</sup>Sr isotope correlation diagram

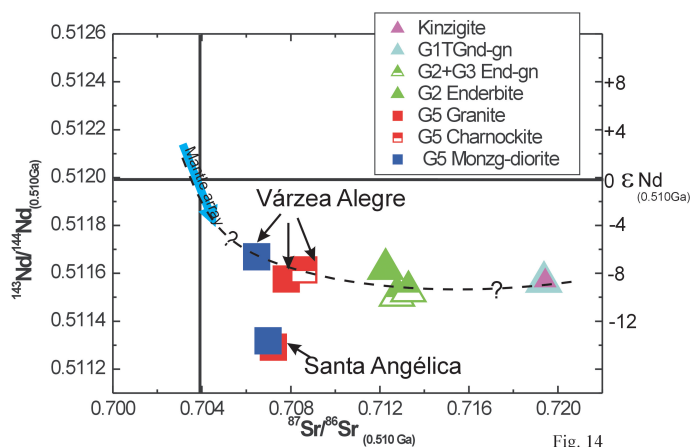


Fig. 14

Source of data in Table 1 . Explanation in text.

Geothermometry using orthopyroxene-garnet and orthopyroxene-clinopyroxene pairs and geobarometry using orthopyroxene-garnet-plagioclase-quartz, yield metamorphic conditions up to 750°C and pressures between 3-4 kb to 6.9 kb for G2 enderbite rocks (Sluitner, 1989).

In summary, the whole package of sediment-derived gneisses of the Paraíba do Sul unit underwent successive partial dehydration melting episodes, probably according to the following reaction: biotite + plagioclase + quartz = K-feldspar + orthopyroxene + garnet + cordierite + spinel + melt (Montel & Vielzeuf, 1997; Brown, 2001; Rushmer, 2001). In an early stage, anatexis I originated G2 granitoids at 575 ± 2 Ma, which included contribution of lower crustal melts (Sluitner & Weber-Diefenbach, 1989). This was followed by anatexis II from 565 to 558 Ma, when the rock package crossed once more the solidus curve (ptigmatic folding) under mostly dry granulitic and moderate to low pressure conditions (from P ~3-4 to ~ 6.5 kb; Sluitner, 1989). This phase gave rise to G3 augen gneisses, granitoid gneisses and enderbite gneisses. The presence of heterogeneous metamorphic banding, frequent interbedded calc-silicate lenses, geochemical and isotopic data, point towards a common primary supracrustal origin for both G2 and G3 suites (Söllner et al, 2000; Wiedeman et al., 2002). P-T differences between different partial melting episodes and the contribution of other source materials may explain chemical variations between G2 and G3. Back reaction between the granulitic package and H<sub>2</sub>O-rich fluids, still present in the crust, produced local retrometamorphism. This induced the replacement of pyroxenes by biotite and

the development of symplectitic and coronitic textures in granulitic/enderbitic rocks (Sluitner, 1989; Wiedemann et al., 1997). The final thermal event in the region took place in the interval between 500±15 Ma (U-Pb in zircon) and 492±15 Ma (U-Pb in titanite). These youngest ages are related to the granitic plutonism in this area (Alfredo Chaves-Iconha pluton; Fig. 4).

## The late post-collisional magmatism

After the collisional phase a relative high heat flow rate was maintained in the lower and middle crust (until ca. 560 Ma; Söllner et al. 2000; Pedrosa Soares et al., 2001). From 560 to 535 Ma there seems to have occurred a tectonic relaxation along the entire belt, save for some local movements along ductile shear zones and slight refolding of regional fold. This tectonic break is also followed by a break in the magmatic activity. A new magma influx started around 535 Ma and lasted until 480 Ma defining the G5 late post-collisional suite.

What kind of geological mechanism could have caused such an interruption and then its continuation as a prominent bimodal magmatic activity? This section summarizes the literature aimed at answering this question.

G5 is comprised of several complexly zoned plutons (unit 10 in Figure 2) intruded high-grade gneisses at high angles to the foliation of the enclosing rocks (Figure 15). This suite is characterized by compositions varying from orthopyroxene-gabbro to granite and corresponds to the latest magmatic event of the orogen. One of the most outstanding features of these plutons is the widespread evidence of magma mingling. The deep erosion levels in the region, together with vertical exposures of over 500 m reveal the internal structure of the plutons.

**Figure 15. Várzea Alegre and Santa Angélica Intrusive Complex**

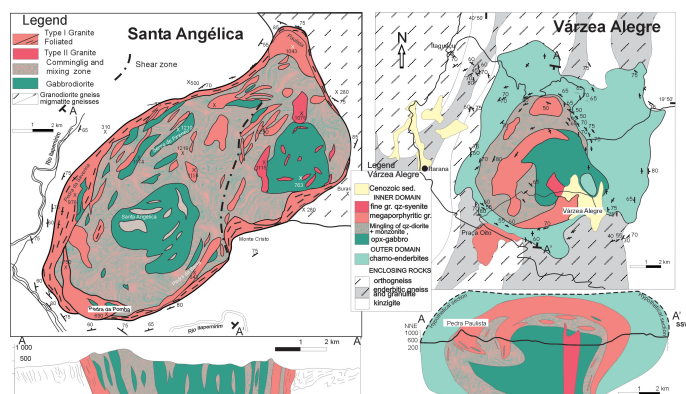


Fig. 15

Várzea Alegre and Santa Angélica Intrusive Complex. Geology of VAIC by Medeiros; Mendes and Wiedemann. Geology of enclosing rocks of VAIC from Tuller (1993). Geology of SAIC from Bayer et al. (1987).

## Geology of the plutons

### Várzea Alegre

The Várzea Alegre Intrusive Complex (VAIC) is an almost circular pluton of approximately 150 km<sup>2</sup> (Figure 15). It shows an inversely zoned structure, with gabbro and diorite in the center, surrounded by coarse-grained granite and an outer domain of megacrystic dark green charnockitic rocks towards the borders [Mendes et al., 1997, 1999; Medeiros et al, 2000, 2001, 2003]. Country rocks are G2 hypersthene-garnet-plagioclase granulites and Paraíba do Sul (Ubu series) cordierite-garnet-biotite metasedimentary gneisses with marked NE-SW striking gneissic foliation.

The outer domain of the intrusion consists of apatite-zircon-allanite-magnetite-hypersthene-mesoperthite quartz-diorite, granodiorite and quartz-monzonite. The domain varies in width from hundred meters, at the southern and western borders, to almost 4 km, at the eastern and northern borders, forming an expressive topography of 'sugar loaves'. When exposed, the contact to the country rocks is sharp. By contrast, the contact between the charnockites and the internal gabbro/dioritic/granitic domain is ductile and interfingered (Figure 16). The internal magmatic foliation is steeply to moderately dipping (Figure 15).

**Figure 16. Várzea Alegre Intrusive Complex**

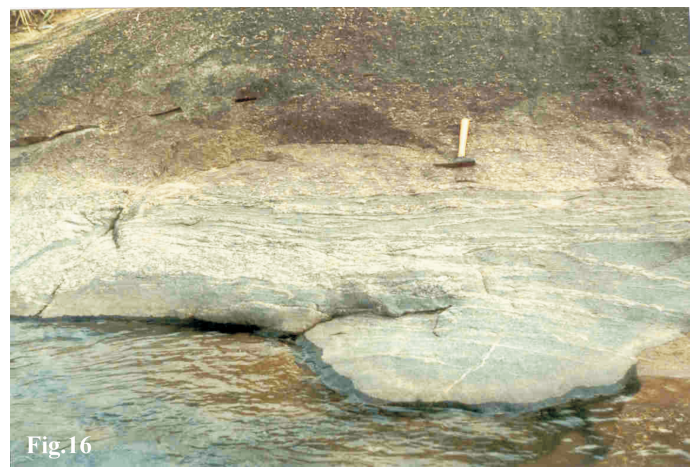


Fig.16

Várzea Alegre Intrusive Complex: interfingering and ductile contact between the charnockite and the internal gabbro/dioritic/granitic domain.

The internal domain consists of a preferentially eroded dark gray apatite-zircon-clinopyroxene (salite-augite)-hypersthene-K-feldspar-plagioclase (An50-65) gabbro/monzogabbro, surrounded by diorite/quartzdiorite-monzodiorite and light megaporphyritic granite (Figure 17). A late stock of sphene-bearing syenogranite cross cuts the orthopyroxene gabbro [Medeiros et al., 2001]. A mingled/mixed zone, consisting of quartz-diorite and quartz-monzodiorite, is characteristic of the contact between the megaporphyritic granite and diorite.

**Figure 17. Foliated coarse grained granite from Várzea Alegre Complex**



Fig.17

Foliated coarse grained granite from Várzea Alegre Complex. K-feldspar grains up to 6 cm.

**Santa Angélica**

The Santa Angélica Intrusive Complex (SAIC, Figure 15) is one of the most interesting examples of the post-collisional plutons in this mobile belt [Wiedemann et al., 1986; Bayer et al., 1987] and 5 Outcrops are described in detail in Appendix 1: Field Guide. The SAIC covers about 200 km<sup>2</sup> and is an elliptical-shaped intrusion composed of several roughly concentric lens-shaped granitic layers, elongated lenses of gabbro-diorite and tightly packed heterogeneous enclave swarms. The complex intrudes an antiformal structure with a northwest plunging hinge, in contrast to other major fold hinges that plunge northeast. The country rocks are high-grade biotite-garnet-sillimanite gneisses (Paraíba do Sul gneiss) and biotite-hornblende granodioritic to tonalitic gneisses (G1 suite). These are locally migmatized, showing sub-vertical concordant foliation to the borders of the intrusive complex, which dip inwards towards the intrusion. The intensity of migmatization is stronger close to the pluton contact, where the gneisses exhibit nebulitic fabrics consistent with partial melting (Figure 18).

**Figure 18. Schematic drawing of the contact between the Santa Angélica Intrusive Complex and the enclosing gneisses**

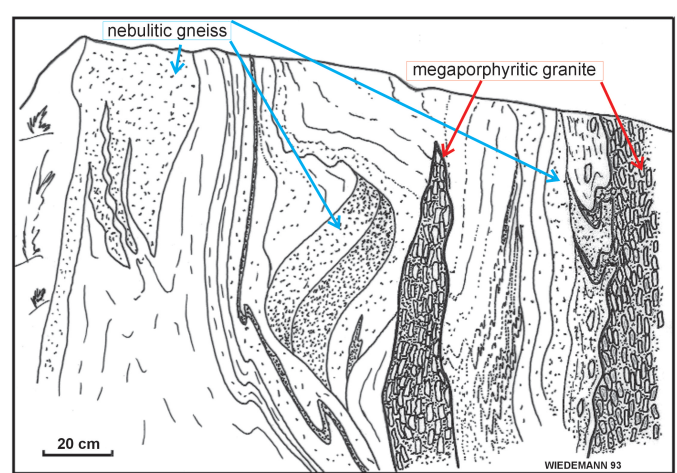


Fig. 18

Schematic drawing of the contact between the Santa Angélica Intrusive Complex and the enclosing gneisses. The intensity of migmatization is stronger close to the pluton contact, where the enclosing gneisses exhibit nebulitic fabrics consistent with partial melting. Redrawn after Schmidt-Thomé (1987).

This intrusion has a general inverse concentric zonation, with more acidic rocks (Type I granite) at the margins,

varying to a twin core of more basic rocks. Type II granite is fine-grained and intruded type I granite through brittle fractures ( Figure 19 ). Magma mingling between monzogabbros and granites can be observed throughout the intrusion (Schmidt-Thomé & Weber-Diefenbach, 1987; Bayer et al., 1987) forming large mingled zones of enclave swarms in different degrees of hybridization with the granite ( Figure 20 and 21 ). A main NE-SW shear zone caused more intensive mingling, producing a fine-banded rock consisting of gabbrodioritic and granitic layers ( Figure 22 ). This NE-SW shear zone separates the two gabbroic nuclei. The foliation inside the intrusive complex trends NE and is normally sub-vertical and, at map scale, the whole magmatic body appears boudinaged.

**Figure 19. Type-I granite intruded by type-II granite at the northwest border of the SAIC**

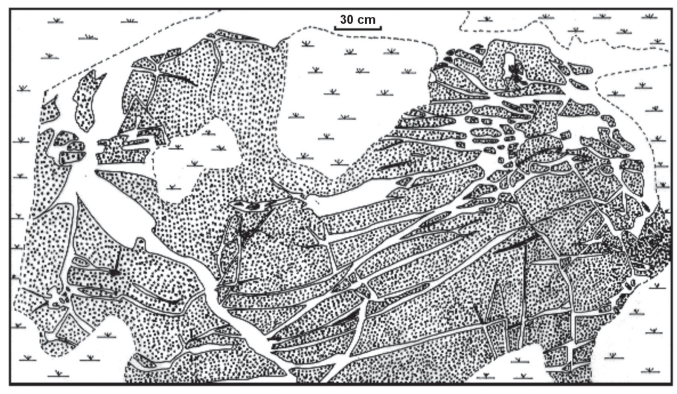


Fig. 19  
 Type-I granite intruded by type-II granite at the northwest border of the SAIC. Drawing after photography.

**Figure 20. Large mingled zones**

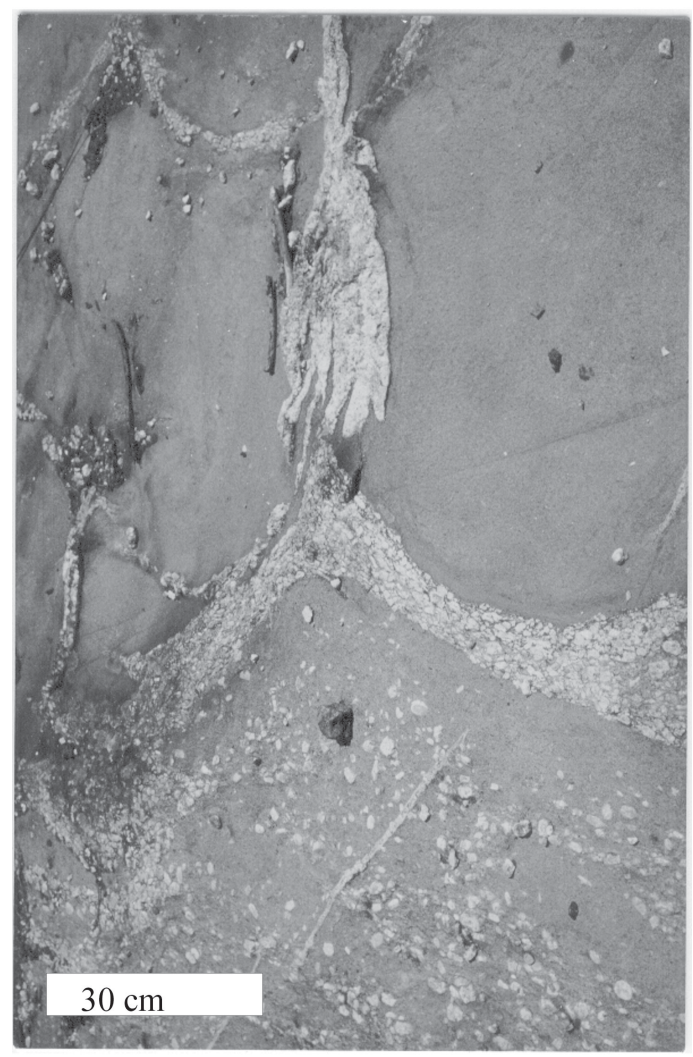


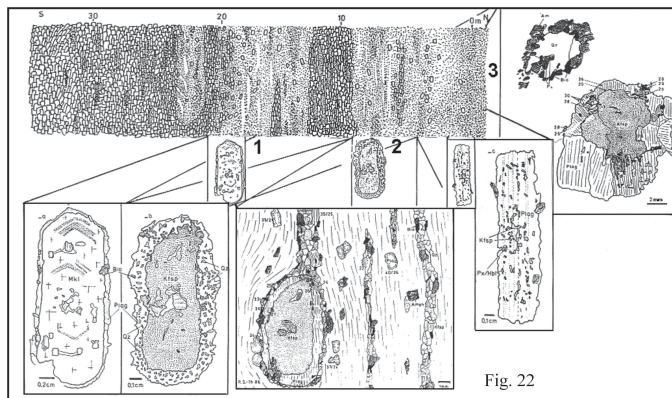
Fig.20  
 Large mingled zones formed by enclave swarms in different degrees of hybridization with the granite (SAIC).

**Figure 21. Complexly mantled feldspar and quartz crystals (SAIC)**



Complexly mantled feldspar and quartz crystals (SAIC).

**Figure 22. Schematic representation of a hybrid zone in SAIC**



Schematic representation of a hybrid zone in SAIC (Lambari Frio region). Fine-banded rock, consisting of gabbrodioritic and granitic layers, cropping out along this main NE-SW shear zone. Schlieren of coarse-grained allanite-granite interfingered with dioritic magma. In the hybrid zone of granodioritic composition, three main types of mantled feldspars are found: 1) soft corroded with microcline cores and oligoclase borders; 2) orthoclase cores and plagioclase borders. Small numbers are anorthite-contents of border and matrix plagioclase; 3) corroded plagioclase from the dioritic layers. Associated with this third type there are quartz xenocrysts mantled with mafic minerals, such as amphibole and biotite. Feldspar aggregates are also common in this zone. Schematic drawing after Schmidt-Thomé (1987).

Structural studies along the contact with country rocks [Bayer, 1987; Wiedemann et al., 1997] point towards a possible ascent as a diapir, partly controlled by shear zones [Weinberg et al., 2004]. A possible explanation for the lack of a marginal syncline related to downward movement of

country rocks responding to an upward rising of a diapir, could be the contemporaneous migmatization of a previously isoclinally folded crust during magma ascent. However, local small scale synclines have been observed along the contacts as shown on Figure 18 .

**Castelo**

The Castelo Complex ( Figure 23 ) is an elliptical intrusion ~ 100 km<sup>2</sup> with a dioritic center and a granitic border. The outermost plutonic unit is over 2 km wide and consists of interlayering between two granite types: a megaporphyritic monzogranite and a fine-grained monzogranite showing well-defined foliation. The fine-grained granite is also porphyritic and sphene-bearing. It is very similar to the type-II granite from Santa Angélica. Micaeous schlieren and ghost structures, from the partially melted or assimilated metacountry gneisses, are frequently observed in this granite. Intrusive contacts with the border gneiss are lit par lit sills or discordant, as dykes of the fine-grained granite intrude ductile shear zones ( Figure 23 ). The contacts usually show evidence of a stoping mechanism and in all produces an agmatic structure generally with sharp discordant contacts with the enclosing rocks. However, at the regional scale the foliation in the gneissic country rock is broadly concordant with the pluton shape.

**Figure 23. Geological map of Castelo Complex**

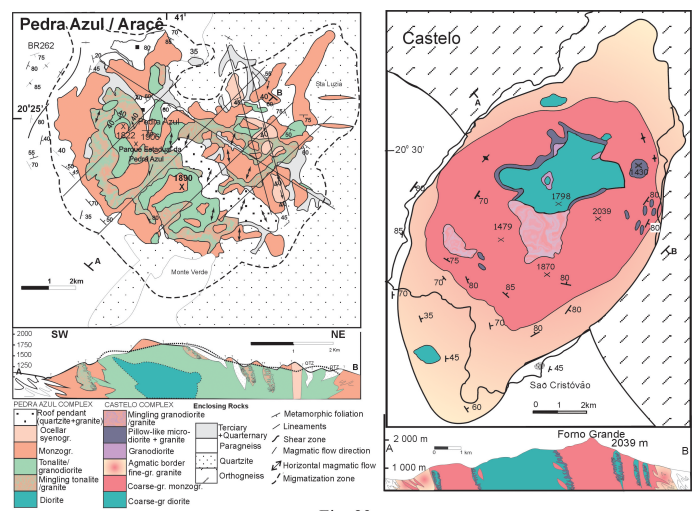


Fig. 23

Geological map of Castelo Complex (by Weinberg, Ludka, Mendes, Horn and Wiedemann. Pedra Azul Complex (by Costa Nascimento, Costa-de-Moura and Wiedemann). References in text.

The core of the intrusion consists of a coarse-grained diorite. From the border towards the core there is a decrease

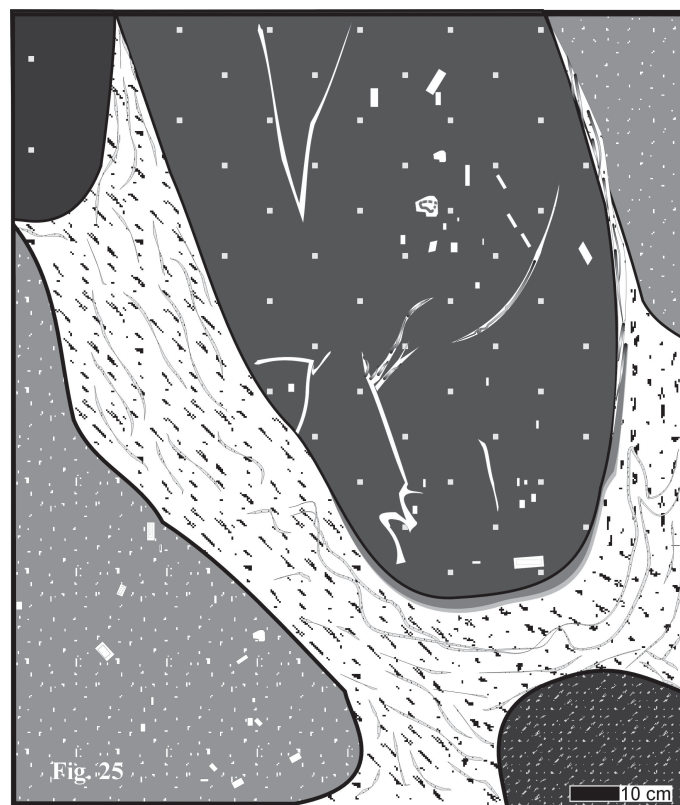
in intensity of magmatic foliation. Joints filled with granitic veins is typical of the core region and suggests fracturing and dyking of an early consolidated dioritic body, possibly due to shrinkage during solidification (Wiedemann et al., 1997). The contact between granite and diorite is a narrow zone, ~ 100 m wide, formed by microgranular enclave swarms mixed to different degrees with granite ( Figure 24 ). In this zone quartz xenocrysts with hornblende and/or biotite rims (quartz ocelli), such as those found in Santa Angélica ( Figure 25 ), feldspars showing antirapakivi- and rapakivi-type mantling are also common. In contrast to the Santa Angelica Complex, mingling in Castelo was between granite and diorite instead of gabbro. Another typical attribute for the hybrid zone in Castelo are spotted textures (Hibbard, 1995) and the presence of granitic schlieren in the microdiorite.

**Figure 24. In the Castelo Complex**



In the Castelo Complex, type-II, 10cm-wide, granite dyke (obliquely N-S in the figure) intrudes the border gneiss, along a ductile shear zone seen displacing and shearing a mafic band in the gneiss (obliquely E-W). Granite dyke is highlighted with yellow and black contour.

**Figure 25. Contact between granite and diorite is a narrow zone**



In the Castelo Complex, the contact between granite and diorite is a narrow zone ~ 100m wide, consisting of microgranular enclave swarms in different mingling degrees with the granite. Different grey patterns represent mafic pillows of different compositions, resulting from different mixing degrees with granite. Notice mantled feldspar phenocrysts in the mafic pillows. The white lines in the pillow on the upper side of the figure represent local granitic melt segregations, while the gray lines in the granitic matrix indicate the main flow directions. Drawing after a photograph.

Compared to the Santa Angelica Complex, the Castelo Complex shows less plastic strain, which, together with the evidence for stoping along the margins, might indicate different emplacement regimes or different intrusion levels.

**Pedra Azul**

The Pedra Azul Complex (PAC, Costa-de-Moura et al., 1999) is an irregular intrusion covering close to 200 km<sup>2</sup>. It is formed by mingling of contrasting magmas, grading from diorite to a medium-grained syenogranite ( Figure 23 ). A general NW-SE and NE-SW fracturing is observed along the whole pluton and its sillimanite quartzites and aluminous gneisses wall rocks. The igneous lithotypes are separated from the enclosing rocks by a migmatized zone,

which shows stoping, lit-par-lit intrusion or nebulitic contacts, with widespread partial melting of the metamorphic units. Megaporphyritic or coarse-grained facies, such as those found in most other plutons are absent in this intrusion. A medium-grained monzogranite forms the highest peaks in the center and lower border regions, constituting the outermost magmatic envelope of the structure [Wiedemann et al., 2002]. Domains of tonalitic to granodioritic compositions crop out in the center of the pluton. The contact between the monzogranite and the tonalitic to granodioritic domains is marked by mingled zones, where granitic schlieren, in contact with more mafic- and finer-grained rocks, originate pillow-like and net-veined structures. A small region of dioritic composition is exposed over 6 km<sup>2</sup>, at the northern border, close to the city of Aracê. The igneous flow in the PAC is marked by magmatic lineation and by the alignment of enclaves as indicated in the map in Figure 23 (Costa-de-Moura et al., 1999).

Abundant host rocks slabs and smaller xenoliths of sillimanite quartzite and garnet-sillimanite-biotite gneiss define an agmatitic mixture of granitic veins and xenoliths, cropping out over some 15 km, in a 1 km-wide zone in the interior of the pluton. This zone follows a SE-NW lineament (fracture or fault zone), crosses almost the entire pluton and is interpreted as an assimilated roof pendant (see "Roof pendant" in Figure 23), from the uppermost part of the structure. Several bands of country rocks swarms in the granite domain have been described mostly parallel to the NW border.

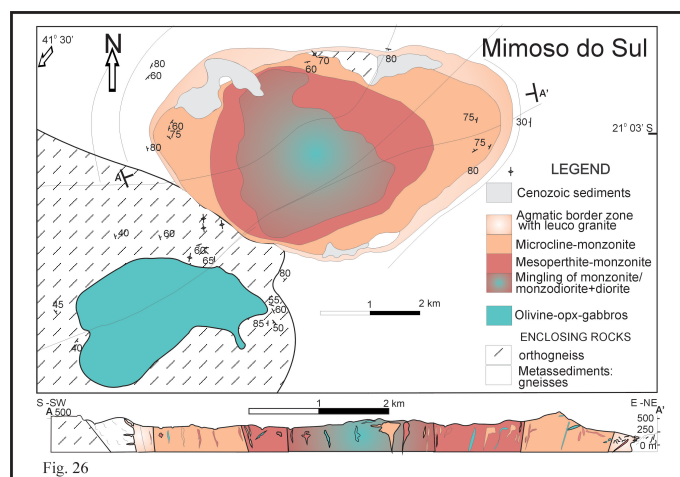
The last intrusive event in the PAC was the emplacement of several stocks of ocellar syenogranite, elongated along a NW-SE fracture zone. The ocellar texture of this late syenogranite is a peculiar one and is formed by hololeucocratic (quartz and K-feldspar), titanite-rich spots, wrapped by a biotite-magnetite-ilmenite-rich mesocratic matrix, in which allanite and titanite are present.

The magnitude of the magnetic anomaly (Tuller, 1993), corresponding to the intrusion of Pedra Azul, is comparable to that of Santa Angélica. However, the small amount of Outcropping basic rocks, together with the presence of a large sillimanite-quartzite roof pendant, indicate shallower erosion and/or lower intrusion levels at Pedra Azul. Compared to the other intrusive complexes, Pedra Azul has the largest volume of hybrid rocks.

### Mimoso do Sul

The Mimoso do Sul Complex consists of two separate intrusions: a predominantly monzonitic unit (Torre Pluton) and a gabbroic unit (Jacutinga Pluton) (Figure 26). The Torre Pluton has three concentric layers: 1) a center of dioritic /monzodioritic composition; 2) a ring of mesoperthitic monzonite; and 3) an outer ring of microcline-quartzmonzonite and granite. The contact between the pluton and the enclosing rock is sharp. Inside the pluton, the gradual change from microcline quartzmonzonite towards the dioritic/monzodioritic center could only be traced by detailed petrographic mapping (Ludka, 1991). In the Torre Pluton the magmatic foliation is steep to sub-vertical. Associated sills or dykes of peralkaline apatite-biotite-Fe-augite pyroxenites crosscut the outer border and the center of the intrusion.

Figure 26. Geological map of the Mimoso do Sul Complex



Geological map of the Mimoso do Sul Complex, by Ludka, and Wiedemann. References in text.

The gabbroic body of the Jacutinga Pluton consists of gabbro-noritic rocks with compositions grading from fine-grained olivine-orthopyroxene(opx)-clinopyroxene(cpx) melagabbros up to coarse-grained opx-cpx leucogabbros. Fine igneous layering (Figure 27) is characteristic for most Jacutinga Outcrops. Coronitic textures, consisting of complex olivine-(and/or pyroxene)-plagioclase overgrowths or intergrowths, are also common (Ludka, 1991; Wiedemann et al., 1995; Ludka, 1997).

**Figure 27. Fine rhythmic layering in the monzodiorite from the Torre Pluton**



Fine rhythmic layering in the monzodiorite from the Torre Pluton, consisting of primary mesoperthite+plagioclase+clinopyroxene+biotite+apatite. This feature is also characteristic for most Jacutinga Pluton Outcrops, in Mimoso do Sul.

### **Geochemistry and Geochronology of the Late Post-Collisional Magmatism**

Three distinct magmatic suites have been recognized in the G5 group (Figure 10 b and 11b; Wiedemann et al, 1986; Horn & Weber-Diefenbach, 1987; Offman, 1990; Ludka, 1991; Wiedemann, 1993; Mendes et al, 1997; Medeiros et al., 2001; Wiedemann et al., 2002): a) tholeiitic (Jacutinga and Itaoca), b) high-K calc-alkaline (Santa Angélica, Castelo, Iconha, Pedra Azul, Várzea Alegre), and c) a very high-K alkaline (Torre/Mimoso do Sul, Venda Nova and Conceição de Muqui). The use of shoshonite as a classification for the very high-K suite has been avoided because this term has been proposed for a volcanic rock, a trachyandesite (Iddings, 1982). The granitoids focused here are usually coarse-grained and very rich in feldspar. In this case very high-K contents could be the result of feldspar accumulation processes. Examples of whole-rock geochemical analyses of the G5 group are presented in Tables 2 and Table 3. The high-K calc-alkaline rocks (suite b) above) are the most significant group (almost 90% of all plutons, by area and volume) while suites a) and c) are restricted (Fig. 2).

G5 high-K calc-alkaline granitoids plot in the R1R2-diagram (Fig. 9c,d; Batchelor & Bowden, 1985) from field 2 (pre-plate collision) and field 6 (syn-collision and anatectic melts) towards field 3 (post-collision uplift). Very

high-K granitoids (suite c) plot mainly in the late-orogenic field 4. Comparison between G1, G2, G3 and G5 (Fig. 9a,b), suggests a gradational change in composition with time, typical for younger orogenic belts (Bonin, 2004). While G5 granitoids plot mostly in fields 3 and 4 for late orogenic plutons, with less evolved compositions in field 2, for pre-plate collision magmas, the older G1 and G2 - G3 suites tend to concentrate in fields 2 and 1+2, respectively.

Most granitoids are abnormally enriched in incompatible elements, mainly LILE, such as K, Ba, Sr and LREE (Figure 12b and 28). High contents of HFSE, Ti, Y, Nb, P and Zr (Horn & Weber-Diefenbach, 1987; Tables 2 and 3) are also characteristic. REE diagrams from several G5 intrusions are shown in Figure 28. Almost all units from Iconha (not described here) and Venda Nova Plutons/Complexes show similar variations in chondrite-normalized REE distributions, with steep slopes from LREE to HREE (Figure 28 c). The more evolved granite II have lower LREE/HREE ratios (Figure 28 c,d), commonly observed in high-silicate magmas. This may be attributed to fractionation of accessory phases (e.g. zircon, monazite, allanite - DePaolo, 1988). Regarding the least evolved rocks, Jacutinga gabbro-norites show gentle slopes (Figure 28 a) while the monzogabbros at Venda Nova and monzodiorites at Iconha (Figure 28 b,c,d) have much steeper patterns. When comparing the least evolved rock associations from these plutons, it is evident that, although Jacutinga rocks show strong enrichment in incompatible elements (Figure 28 a) those from Venda Nova (Figure 28 b,c) are more enriched. Jacutinga gabbro-norites contain hypersthene and no alkaline minerals, not even in the CIPW-norm. Olivine is restricted to a local occurrence. The rocks from Torre and Venda Nova bodies, on the other hand, have much higher K<sub>2</sub>O-contents for lower SiO<sub>2</sub>-values (Figs 9c,d and 11B). This results in the absence of hypersthene in most lithotypes, crystallization of Fe-salite instead, presence of leucite in the CIPW-norm and agpaitic index > 1 (Ludka, 1997). Therefore the Torre Pluton and Venda Nova Complex are considered to be examples of the onset of a late-orogenic alkaline magmatism. This is a gradual process with the coeval intrusion of peraluminous calc-alkaline granites from crustal remelting (Figure 10 B), which are usually found associated with the alkaline/peralkaline lithotypes (monzonites, monzodiorites and associated pyroxenite/biotitite of Figs 9D and 26).

**Figure 28. Rare Earth Element abundance normalized to chondrite**

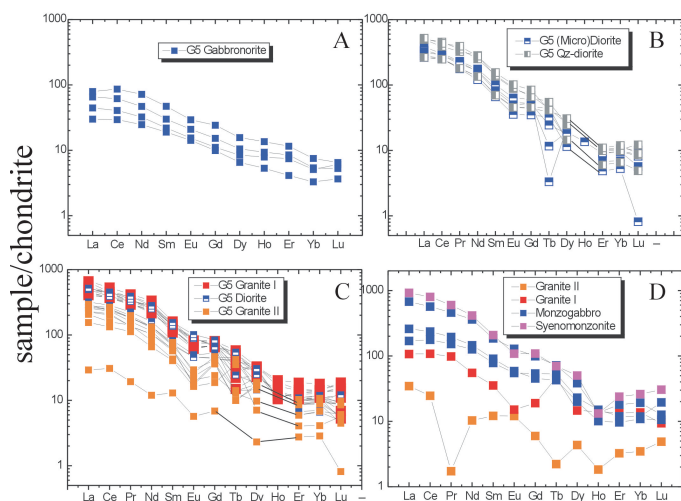


Fig.28 A, B, C D

Rare Earth Element abundance normalized to chondrite (after McDonough and Sun, 1995) plotted against REE atomic numbers. A: G5 gabbronorite from Jacutinga (data from Ludka, 1997). B: G5 microdiorite and quartz-diorite from Iconha (data from Offman, 1990). C: G5 granite I, -granite II and diorite from Iconha (data from Offman, 1990); D) G5 very high-K rocks from Venda Nova (data from Offman, 1990). Discussion in text.

Migmatization of country rocks during emplacement could account for similarities between REE patterns of enclosing gneisses and G5 granites (granite II; Figure 13 and 28). However, the Nd values for Santa Angelica ( Figure 14 ) show a discrepancy and point towards an older continental source for these granites. The dominant granite I is SiO<sub>2</sub> oversaturated. This granite shows normative corundum and typically high P, Ti, Zr, K, Ba and Sr ( Figure 12 b). Less enriched REE-patterns however similar to those from gabbro-dioritic lithotypes are compatible with a long lasting melt interaction between less and more evolved melts ( Figure 28 b,c,d). LREE contents ( Figure 28 c,d), Rb, Sr and Rb/Sr values are yet typical of the upper crust (Tables 1 and 3) and indicative of a hybrid origin.

Zircon ages constrain the magmatic crystallization of the late plutons to between 530 and 480 Ma (Table 1; Söllner et al., 2000) confirming their late post-collisional emplacement. Units from the Santa Angélica and Mimoso do Sul Complexes yielded the following U-Pb ages: 513±8 Ma, for the Santa Angélica megaporphyritic granite, 492 ±15 Ma for the Santa Angélica type-II titanite granite and 480±4 Ma for the Mimoso do Sul coarse grained

syenomonzonite. Rb-Sr data from the Várzea Alegre megaporphyritic granite yield a whole-rock isochron age of 508 ±12 Ma (Medeiros et al., 2000). Zircons of the charnockitic rocks from Várzea Alegre yielded an U-Pb age of 499±5 Ma, implying that both charnockite and porphyritic granite crystallized simultaneously (Medeiros et al., 2003). Whole-rock Rb-Sr isotopic data from the Pedra Azul granite (Platzer, 1997) indicate a crystallization age of 536 ±31 Ma.

Isotopic data from metabasic rocks from the rifting stage of the orogen point towards a depleted mantle source (Sm-Nd whole-rock isochron based on five samples yielded an age of 816 ± 72 Ma, Nd(t)= +3.4 to + 4.6; Pedrosa-Soares et al., 1998). During the subduction phase of the orogen, repetitive episodes of crustal contamination of the asthenospheric mantle wedge must have occurred to contribute for the enrichment patterns of the intermediate and basic mantle-derived melts. However Nd(t) values below -20 for the Santa Angélica basic rocks (Table 1) together with extremely high Ba and Sr values ( Figure 12 a,b) have been considered to be due to a locally abnormal mantle enrichment (Wiedemann et al., 1995; Ludka et al., 1998).

Figure 14 shows the initial Nd and Sr isotopic compositions for magmatic and metamorphic rocks from the area, time-corrected for the mean crystallization age of the G5 suite (510 Ma). We distinguish two groups, both of which plot in the enriched mantle field. The first group is represented by gabbro, granite and charnockite from Várzea Alegre, by 560 to 580 Ma old metaplutonic rocks of G1 and G2 suites and by the enclosing metasedimentary rocks (>613 Ma kinzingite). This group of samples is characterized by a relatively uniform Nd isotopic composition followed by extreme variations in Sr isotopes. Thereby, the metasedimentary rocks represent the most enriched member. We tentatively interpret this systematics as reflecting contamination of a mantle-derived basaltic melt, now most closely approached by the Várzea Alegre gabbro, due to assimilation of melts derived from a Neoproterozoic crust. In such a model, a hyperbolic mixing curve would start in a more depleted mantle field.

A second group is represented by only two magmatic samples from Santa Angélica, with almost identical Sr-Nd isotopes. U-Pb dating of zircons from these samples indicate zircon cores older than 2000 Ma, possibly Archean (Söllner et al., 1991). Accordingly, the Nd isotopes indicate assimilation of a much older crust than in the case of Várzea Alegre or melt generation from an anomalous enriched

mantle source (Horn & Weber-Diefenbach, 1987; Offman, 1990; Ludka, 1997). Taking into account the reduced number of measured samples, this comparison demonstrates that different plutons may have different magmatic sources. We speculate that the granitic melt from Santa Angélica could have been originated from the melting of an Archean crustal segment. This granitic melt mixed with a mantle derived basaltic melt to produce a hybrid monzogabbro with the same isotopic signature. The smaller spreading of data points between granite and monzogabbro samples, in the Santa Angélica Intrusive Complex, in comparison to Várzea Alegre, is consistent with field and petrographic evidence of a more effective mixing between gabbro and granite in this intrusion. However, high K<sub>2</sub>O-values of most basic and intermediate rocks, and compositional gaps on geochemical trends reflect heterogeneous mingling and restricted mixing. An alternative could be that mixing with a granitic magma may have occurred at depth and high temperature, before plagioclase crystallization, followed by mingling during emplacement, as demonstrated by van Westrenen (1997), using trace element partitioning between plagioclase and less evolved melts from the Pedra Azul Complex.

Magma mingling/mixing, fractional crystallization and assimilation of country rocks are the main differentiation processes during the evolution of these igneous sequences (Wiedemann, 1993; Horn & Weber-Diefenbach, 1989; Mendes et al., 1997, 1999; Platzer, 1995; Mendes et al., 1997; Ludka et al., 1998; Pedrosa-Soares et al., 2001; Medeiros et al., 2000, 2001; Wiedemann et al., 2002). The late post-collisional magmatism is a product of a bimodal system consisting of mantelic and crustal-derived magmas, which are thought to be the end-members of the initial bimodal system. The ascent of mantelic magmas, probably along ductile shear zones, increasing the geothermal gradient, seems to have induced crustal melting. Physical and chemical interaction between these melts at source, separate geochemical evolution in a later stage and restricted hybridization during emplacement could explain the formation of the differently complex zoned plutons. The differences in exposed rock types and in the intensity of magma mingling/mixing processes in the area have been considered to be due to different sources, emplacement conditions and erosional levels (Wiedemann et al., 2002).

The observations summarized here confirm the classical model of generation of granitic and intermediate magmas, induced by underplating of basaltic magma under the

continental crust during late orogenic stages (Batchelor & Bowden, 1985; Hall, 1987; Huppert & Sparks, 1988; Bonin, 2004; Perugini et al., 2004).

## Conclusion

The southern Espírito Santo region is a segment of the Araçuaí-Ribeira - West-Congo foldbelt. The main collisional and deformational stage of the Brasiliano orogen, in this region, lasted from ~ 600 to 580 Ma. During this collisional episode folding and thrusting caused considerable crustal thickening and metamorphism increased up to high amphibolite and granulite facies, overprinting older structures.

In the central region of the belt, the intrusion of large batholiths of mainly tonalitic magmas (Fig. 9b) took place ~10 Myr after the amphibolite to granulite facies metamorphism, originating biotite ± hornblende ± plagioclase ± garnet ± hypersthene gneisses (G1 suite). These magmas intruded a thick continental crust of mostly pelitic composition with minor carbonate - and quartz-rich sequences (Paraíba do Sul Complex - Ubu series), characterizing distant and proximal marine environments, respectively.

This thick continental crust underwent different ultrametamorphic conditions in different regions of the belt. While the westernmost granulites from the Caparaó Ridge (Figure 2 and 3) crystallized under P-T conditions exceeding 10 kb and 800 °C, along the Atlantic coast, the Costeiro Complex shows younger ages. There, P-T conditions remained lower, around 7.5 kb and below 800 °C (Figure 29). The origin of both high-grade metamorphic rock packages is attributed to a progressive dehydration melting and to the influx of carbonic fluids into the crust [Sluitner & Weber-Diefenbach, 1989; Seidensticker, 1990; Fritzer, 1991; Seidensticker & Wiedemann, 1992]. This process culminated with the crystallization of granodioritic to tonalitic hypersthene gneisses (G2 gneisses and enderbites and G3 enderbitic suites from partial remelting of G2) in the Costeiro Complex. Along the coast this phenomenon took place about 20 Ma later (only around 565 ± 9 Ma) than in the Caparaó region. The granulitization process was followed by widespread migmatization since enough heat was available to cross the solidus for renewed dehydration (Figure 29). Hypersthene-bearing melts crystallized at a concordant U-Pb zircon age of 558 ± 2 Ma (Söllner et al., 1989).

**Figure 29. P-T-diagram showing the approximate conditions**

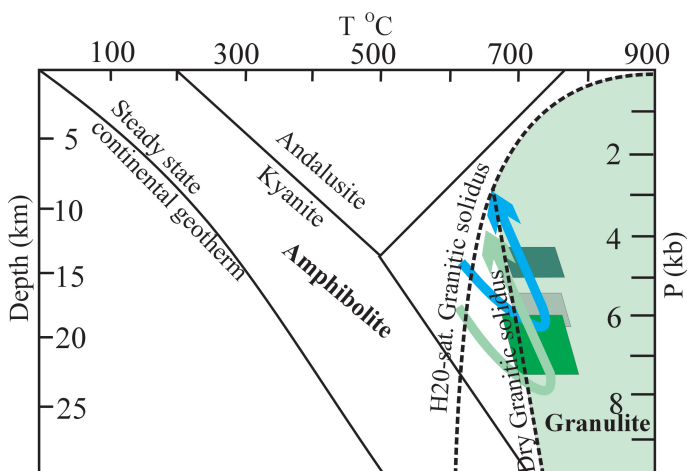


Fig. 29

P-T-diagram showing the approximate conditions range for two different metamorphic paths, followed by anatexis events in the Costeiro Complex (after data from Sluiter, 1989). Geothermometry and barometry using orthopyroxene-garnet and orthopyroxene-clinopyroxene pairs as thermometers and orthopyroxene-garnet-plagioclase-quartz as barometer. The melting/anatexis curve for peraluminous (S-Type) granite under water-saturated conditions is from Clemens and Wall (1981). Steady state continental geotherm and dry granitic solidus curve from Philpotts (1990). Explanation and discussion in text.

During the collision, incompatible elements could have been progressively introduced into the mantle through subduction. When collisional deformation ceased, in Cambro-Ordovician times, remarkable amounts of magma intruded the highly metamorphosed gneisses and granulites, during a final thermal event, around 500 Ma (G5 suite, Wiedemann et al., 2002). These are characterized by mantle

derived mafic magmas with high values of incompatible elements mingled with felsic magmas.

Tholeiitic (Jacutiga Pluton), medium- to high-K calc-alkaline melts (SAIC, Várzea Alegre, Alfredo Chaves - Iconha, Castelo, Pedra Azul Plutons) with gradational changes into alkaline-richer compositions (Venda Nova, Conceição de Muqui and Torre Plutons) intruded along a relative narrow NE-SW trending strip ( Figure 2 ). This suggests a steeply-dipping plate underneath, due to slab break off at the final stage of the orogen (Wiedemann et al, 2002). Mafic magmas derived from previously enriched mantle were emplaced within the lower crust and provided enough heat to cause a third crustal anatexis event recorded particularly clearly at the margins of these late intrusions. Consequent changes in temperature and volatile pressure conditions originated granitic to charnockitic magmas which mingled with mantle melts on their way through the crust.

### Acknowledgements

Our thanks to all graduate and post-graduate students, who participated in this project for the last 20 year, specially to M. L. Santos for processing the Landsat image. We are grateful to Frank Söllner for special geochronology samples and Alexander Rocholl for discussion on the results. The following institutions directly or indirectly supported this research: CNPq, FINEP and CAPES (Brazil), the University of Munich (LMU) and DAAD (Germany) and the University of Utrecht (Netherlands). We are deeply indebted to Roberto Weinberg and to an anonymous reviewer for thoughtful and careful reviews, which greatly improved the first version of this manuscript.

## References

- Almeida, F.F.M., Amaral, G., Cordani, U.G. and Kawashita, K., 1973. The Precambrian evolution of the South American cratonic margin, South of the Amazon River. In: A.E.M. Nair and F.G. Stehli (Editors). *The Ocean Basins and Margins*. New York, Plenum Publ. Co., 1: 411-446.
- Asrat, A., Barbey, P., Ludden, J.N., Reisberg, L., Gleizes, G. and Ayalew, D., 2004. Petrology and isotope geochemistry of the Pan-African Negash Pluton, Northern Ethiopia: mafic-felsic magma interactions during the construction of shallow-level calc-alkaline plutons. *Journal of Petrology*, 45: 1147-1179.
- Batchelor, R.A. and Bowden, P., 1985. Petrogenetic interpretation of granitoid rocks series using multicationic parameters. *Chemical Geology*, 48: 43-55.
- Bayer, P., 1987. *Strukturgeologische Untersuchungen im Brasilianischen Küsten Mobile Belt, südliches Espírito Santo, unter besonderer Berücksichtigung der Brasiliano Intrusionen*. Münchener Geowissenschaftliche Abhandlungen, B/2, München, Friedrich Pfeil Verlag, 144 pp.
- Bayer, P., Horn, H. A., Lammerer, B., Schmidt-Thomé, R., Weber-Diefenbach, K. and Wiedemann, C., 1986. The Brasiliano Mobile Belt in Southern Espírito Santo (Brazil) and its igneous intrusions. *Zentralblatt f. Geologie und Paläontologie*. Teil I, 9/10: 1429-1439.
- Bayer, P., Schmidt-Thomé, R., Weber-Diefenbach, K. and Horn, H.A., 1987. Complex concentric granitoid intrusions in the Coastal Mobile Belt, Espírito Santo, Brazil: the Santa Angélica pluton-an example. *Geologische Rundschau*, 76: 357-371.
- Bonin, B., 2004. Do coeval mafic and felsic magmas in post-collisional to within -plate regimes necessarily imply two contrasting, mantle and crustal, sources? A review. *Lithos*, 78: 1-24.
- Brito Neves, B.B., Campos Neto, M.C. and Fuck, R. A., 1999. From Rodinia to Western Gondwana: an approach to the Brasiliano-Pan African cycle and orogenic collage. *Episodes*, 22: 155-166.
- Brown, M., 2001. Crustal melting and granite magmatism: key issues. *Physics and Chemistry of the Earth, part A: Solid Earth and Geodesy*, 26: 201-212.
- Campos-Neto, M.C. and Figueiredo, M.C.H., 1995. The Rio Doce Orogeny, south-eastern Brazil. *Journal of South American Earth Sciences*, 8: 143-162.
- Castro, A., 1987. On granitoid emplacement and related structures. A review. *Geologische Rundschau*, 76: 101-124.
- Costa Nascimento, R.C., De Moura, J. C., Vriend, S.P., Wiedemann, C.M. and Da Silva, D.M.B., 1996. Geologia e petrografia do maciço intrusivo da Pedra Azul e suas rochas encaixantes. In: 39º Congresso Brasileiro Geologia, Salvador, Bahia, Anais, 1: 96-99.
- Costa de Moura, J., Wiedemann, C.M., Wallffas, C.M. and Van Westrenen, W., 1999. O pluton de Pedra Azul: a estrutura do maciço intrusivo e suas rochas encaixantes- Domingos Martins, ES, Brasil. In: *Simpósio Nacional Estudos Tectônicos, Lençóis, Bahia, Anais: 129-131*.
- Clemens, J.D. and Wall, V.J., 1981. Origin and crystallization of some peraluminous (S-type) granitic magmas. *Canadian Mineralogist*, 19: 111-131.
- Cunningham, W.D., Alkmim, F.F. de. and Marshak, S., 1998. A structural transect across the Coastal Mobile belt in the Brazilian Highlands (latitude 20 S): the roots of a Precambrian transpressional orogen. *Precambrian Research*, 92: 251-275.
- de la Roche, H., Leterrier, J., Grand Claude, P. and Marchal, M., 1980. A classification of volcanic and plutonic rocks using R1-R2 diagrams and major element analyses - its relationships with current nomenclature. *Chemical Geology*, 29: 183-210.
- DePaolo, D.J., 1988. *Neodymium Isotope Geochemistry*. Springer Verlag, 187 pp.
- Delgado, I. and Marques, V.J., 1993. *Programa Levantamentos Geológicos Básicos do Brasil, Folhas Piuma, Cachoeiro do Itapemirim, Afonso Cláudio, Domingos Martins, Baixo Guandu e Colatina. Espírito Santo. Escala 1:100.000, DNPM/CPRM. Brasília, 125 pp.*
- Féboli, W.L., 1993. Explained text of the Folha SF.24-V-A-VI, Piuma. In: M.P. Tuller (Editor). *Programa Levantamentos Geológicos Básicos do Brasil, DNPM/CPRM, Brasília, 114 pp.*
- Fischel, D.P., 1998. *Geologia e dados isotópicos Sm-Nd do Complexo Mantiqueira e do Cinturão Araçuaí-Ribeira na região de Abre Campo, Minas Gerais. Instituto de Geociências, Universidade de Brasília, MSc Thesis (unpublished), 99 pp.*
- Fritzer, T., 1991. *Das Guaçuí Lineament und die orogene Entwicklung des Zentralen Araçuaí-Ribeira Belt (Espírito Santo, Brasilien)* Münchener Geowissenschaftliche Abhandlung, 2, München, Friedrich Pfeil Verlag, 196 pp.
- Geiger, A., 1993. *Die Geologie des Steinbruchreviers von Cachoeiro de Itapemirim Südliches Espírito Santo, Brasilien.* Münchener Geowissenschaftliche Hefte 11, München, Friedrich Pfeil Verlag, 217 pp.
- Hall, A., 1987. *Igneous Petrology*. Longman Sc. and Tech., N.Y., 568 pp.
- Hibbard, M.J. and Watters, R.J., 1985. Fracturing and diking in incompletely crystallized granitic plutons. *Lithos*, 18: 1-12.
- Hibbard, M.J., *Petrography to Petrogenesis*. Prentice Hall, N.J., 587 pp.

- Horn, H.A. and Weber-Diefenbach, K., 1987. Geochemical and genetic studies of three inverse zoned intrusive bodies of both alkaline and subalkaline composition in the Araçuaí-Ribeira Mobile Belt (Espírito Santo, Brazil). *Revista Brasileira de Geociências*, 17: 488-497.
- Huppert, H.E. and Sparks, R.S.J., 1988. The generation of granitic magmas by intrusion of basalt into continental crust. *Journal of Petrology*, 29: 599-624.
- Iddings, J.P., 1982. The origin of igneous rocks. *Bulletin of the Philosophical Society of Washington*, 12: 89-213.
- Irvine, T.N. and Baragar, W.R., 1971. A guide to the chemical classification of the common volcanic rocks. *Canadian Journal of Earth Sciences*, 8: 523-548.
- Lammerer, B., 1987. Short notes on a structural section through the Araçuaí-Ribeira Mobile Belt (Minas Gerais and Espírito Santo, Brazil). *Zentralblatt f. Geologie und Paleontologie, Teil I*, H 7/8: 719-728.
- Le Maitre, R. W. (Editor), 1989. *A Classification of Igneous Rocks and a Glossary of Terms*. Blackwell, Oxford, 193 pp.
- Leonardos, O.H. and Fyfe, W.S., 1974. Ultrametamorphism and melting of a continental margin: the Rio de Janeiro region, Brasil. *Contributions to Mineralogy and Petrology*, 46: 201-214.
- Liégeois, J.P. and Black, R., 1987. Alkaline magmatism subsequent to collision in the Pan-African belt of the Adrasdes Ifora (Malit). In: Fitton, J.G., Upton, B.G.J. (Editors). *Alkaline Igneous Rocks*, Geological Society of London, Special Publication, 30: 381-401.
- Ludka, I.P., 1991. *Geologia, petrografia e geoquímica do complexo intrusivo de Jacutinga-Torre, Mimoso do Sul, Espírito Santo*. MSc Thesis (unpublished), Department of Geology, Federal University of Rio de Janeiro, 256 pp.
- Ludka, I.P., 1997. *Geoquímica do magmatismo básico na porção central do Cinturão Móvel Costeiro e regiões adjacentes aplicada ao estudo da composição do manto (SE Brasil)*. PhD Thesis (unpublished), Department of Geology, Federal University of Rio de Janeiro, 240 pp.
- Ludka, I.P., Wiedemann, C.M. and Töpfner, C., 1998. On origin of incompatible elements in the Venda Nova pluton, state of Espírito Santo, southeast Brazil. *Journal of South American Earth Sciences*, 11: 473-486.
- Ludka, I.P. and Wiedemann, C.M., 2000. Further signs of an enriched mantle source under the Neoproterozoic Araçuaí-Ribeira Mobile Belt. *Revista Brasileira de Geociências*, 30: 95-98.
- Maniar, P.D. and Piccoli, P.M., 1989. Tectonic discrimination of granitoids. *Geological Society of America Bulletin*, 101: 635-643.
- McDonough, W.F. and Sun, S.S., 1995. Composition of the Earth. *Chemical Geology*, 120: 223-253.
- Medeiros, S.R., Wiedemann, C.M. and Mendes, J.C., 2000. Post-collisional magmatism in the Araçuaí-Ribeira Mobile belt: geochemical and isotopic study of the Várzea Alegre intrusive complex (VAIC), ES, Brazil. *Revista Brasileira de Geociências*, 30: 30-34.
- Medeiros, S.R., Wiedemann, C.M. and Vriend, S., 2001. Evidence of mingling between contrasting magmas in a deep plutonic environment: the example of Várzea Alegre in the PanAfrica/Brasiliano Mobile Belt in Brazil. *Anais da Academia Brasileira de Ciências*, 73: 99-119.
- Medeiros, S.R., Mendes, J.C., McReath, I. and Wiedemann, C.M., 2003. U-Pb and Rb-Sr dating and isotopic signature of the charnockitic rocks from Varzea Alegre intrusive complex, Espírito Santo, Brazil. In: IV South American Symposium on Isotope Geology. Short papers. II: 609-612.
- Mendes, J.C., McReath, I., Wiedemann, C.M. and Figueiredo, M.C.H., 1997. Charnokitóides do maciço de Várzea Alegre: um exemplo de magmatismo cálcio-alcálico de alto K no arco magmático do Espírito Santo. *Revista Brasileira de Geociências*, 27: 13-24.
- Mendes, J.C., Wiedemann, C.M. and McReath, I., 1999. Conditions of formation of charnockitic magmatic rocks from the Várzea Alegre massif, Espírito Santo, southeast Brazil. *Revista Brasileira de Geociências*, 29: 47-54.
- Montel, M. and Vielzeuf, D., 1997. Partial melting of metagreywackes: part II. Compositions of minerals and melts. *Contributions to Mineralogy and Petrology*, 128: 176-196.
- Noce, C.M., Pedrosa-Soares, A.C.P., De Campos, C.M. and Medeiros, S.R., 2004. Idades U-Pb (SHRIMP) de zircões detriticos do complexo kinzigítico do norte do Espírito Santo: evidência de sedimentação em bacia de retroarco do Orógeno Araçuaí. In: 42o Congresso Brasileiro de Geologia, Araxá, Anais: 187.
- Offman, R., 1990. *Geologische, petrographische und geochemische Charakterisierung des Intrusivkomplexes von Iconha im südlichen Espírito Santo/ Brasilien unter besonderer Berücksichtigung der Spurenelementpetrologie zur Deutung der Magmengeneese*. PhD Thesis (unpublished). Ludwig-Maximilians-Universität, München, 204 pp.
- Pedrosa-Soares, A.C., Vidal, P., Leonardos, O.H. and Brito-Neves, B.B., 1998. Neoproterozoic oceanic remnants in eastern Brazil: further evidence and refutation of an exclusively ensialic for the Araçuaí-West Congo orogen. *Geology*, 26: 519-522.
- Pedrosa-Soares, A.C., Wiedemann, C.M., Fernandes, M.L.S., Faria, L.F. and Ferreira, J.C.H., 1999. Geotectonic significance of the Neoproterozoic granitic magmatism in the Araçuaí belt, Eastern Brazil: a model and pertinent questions. *Revista Brasileira de Geociências*, 29: 59-66.

- Pedrosa-Soares, A.C. and Wiedemann-Leonardos, C.M., 2000. Evolution of the Araçuaí Belt and its connection to the Araçuaí-Ribeira Belt, eastern Brazil. In: Cordani, U.G., Milani, E.J., Thomaz Filho, A. and Campos, D.A. (Editors), *Tectonic Evolution of South America*, 31st IGC: pp. 265-285.
- Pedrosa-Soares, A.C., Noce, C.M., Wiedemann, C.M. and Pinto, C.P., 2001. The Araçuaí-West Congo orogen in Brazil: an overview of confined orogen formed during Gondwana assembly. *Precambrian Research*, 110: 307-323.
- Perugini, D., Poli, G. and Bonin, B., 2004. Interaction between mafic and felsic magmas in orogenic suites. *Lithos*, 78: ix-xii.
- Philpotts, A.R., 1990. *Principles of Igneous and Metamorphic Petrology*. Prentice Hall, N.J., 498 pp.
- Platzer, S., 1997. Whole rock geochemistry of the Aracê/Pedra Azul pluton. MSc Thesis (unpublished), University of Utrecht, 58 pp.
- Rajesh, H.M., 2004. The igneous charnockite-high-K alkalic-calcic I-type granite-incipient charnockite association in Trivandrum Block, southern India. *Contributions to Mineralogy and Petrology*, 147: 346-362.
- Rushmer, T., 2001. Volume change during partial melting reactions: implications for melt extraction, melt geochemistry and crustal rheology. *Tectonophysics*, 342: 389-405.
- Shand, S.J., 1943. *Eruptive Rocks*. 2nd Ed., Willey and Sons, N.Y., 120 pp.
- Schmidt-Thomé, R., 1987. Der Santa Angelica Pluton im Araçuaí-Ribeira Mobile Belt, südliches Espírito Santo, Brasilien: Magmenmischung in einem invers zonierten Pluton. Unpub. PhD Thesis. Ludwig-Maximilians-Universität, München, 191 pp.
- Schmidt-Thomé, R. and Weber-Diefenbach, K., 1987. Evidence for frozen-in magma mixing in Brasiliano calc-alkaline intrusions. The Santa Angélica pluton, southern Espírito Santo, Brazil. *Revista Brasileira de Geociências*, 17: 498-506.
- Seidensticker, U. 1990. Petrographie, Geochemie, Strukturgeologie und Untersuchungen von fluiden Einschlüssen in granulitfaziellen Gesteinen im Suedwesten des Bundesstaates Espírito Santo, Brasilien. Unpub. PhD Thesis, Ludwig-Maximilians-Universität, München, 168 pp.
- Seidensticker, U. and Wiedemann C., 1993. Geochemistry and origin of lower crustal granulite facies rocks, in the Serra do Caparaó region, Espírito Santo/Minas Gerais, Brazil. *Journal of South American Earth Sciences*, 6: 289-298.
- Siga Jr, O., Teixeira, W., Cordani, U.G., Kawashita, K. and Delhal, J., 1982. O padrão geológico-geocronológico das rochas de alto grau da parte setentrional da faixa Ribeira, a norte do Estado do Rio de Janeiro, Brasil. In: Congresso Latinoamericano de Geologia, Buenos Aires, Acta I: 349-370.
- Schobbenhaus, C., Campos, D. de A., Derze, G.R. and Asmus, H.E., 1984. *Geologia do Brasil. Texto Explicativo do Mapa Geológico do Brasil e Área Oceânica Adjacente*. DNPM-Brasília, 78 pp.
- Sluitner, Z., 1989. Petrographie und Geochemie von hochgradig metamorphen, suprakrustalen Gesteinsserien des Brasiliano im suedlichen Espírito Santo/Brasilien unter besonderer Beruecksichtigung der enderbitischen Gesteine. PhD Thesis. Ludwig Maximilians University, Munich, 192 pp.
- Sluitner, Z. and Weber-Diefenbach, K., 1989. Geochemistry of charnoenderbitic granulites and associated amphibolitic gneisses in the coast region of Espírito Santo, Brazil. *Zentralblatt f. Geologie und Paleontologie. Teil I, H. 5/6*: 917-931.
- Söllner, F., Lammerer, B. and Weber-Diefenbach, K., 1989. Brasiliano age of a charnoenderbitic rock suite in the Complexo Costeiro (Ribeira Mobile Belt), Espírito Santo, Brazil: evidence from U-Pb geochronology on zircons. *Zentralblatt f. Geologie und Paleontologie, Teil I, H 5/6*: 933-945.
- Söllner, F., Lammerer, B. and Weber-Diefenbach, K., 1991. Die Krustenentwicklung in der Küstenregion nördlich von Rio de Janeiro/Brasilien *Münchener Geowissenschaftliche Hefte* 11, München, Friedrich Pfeil Verlag, 4, 100 pp.
- Söllner, H.S., Lammerer, B. and Wiedemann-Leonardos, C., 2000. Dating the Araçuaí-Ribeira Mobile Belt of Brazil. In: *Sonderheft, Zeitschrift f. Angewandte Geologie, SH 1*: 245-255.
- Teixeira, A.D., 1998. Mapeamento em detalhe da suite charnoenderbítica do Complexo Costeiro, sul do estado do Espírito Santo. Honours Thesis (unpublished). Department of Geology, Federal University of Rio de Janeiro. 58 pp.
- Trouw, R., Heilbron, M., Ribeiro, A., Paciullo, F., Valeriano, C.M., Almeida, J.C.H., Tupinambá, M. and Andreis, R.R., 2000. The central segment of the Ribeira Belt. In: *Tectonic Evolution of South America*. Cordani, U.G., Milani, E.J., Thomaz Filho, A. and Campos, D.A. (Editors). *Tectonic Evolution of South America*, 31st IGC: pp. 287-310.
- Tuller, M.P., 1993. Texto explicativo da folha SE, 24-Y-C-VI, Colatina. In: Tuller M.P. (org.), *Programa Levantamentos Geológicos Básicos do Brasil*. DNPM/CPRM, Brasília. 163p.
- Tupinambá, M., Teixeira, W. and Heilbron, M. 2000. Neoproterozoic Western Gondwana assembly and subduction-related plutonism: the role of the Rio Negro Complex in the Ribeira belt, southeastern Brazil. *Revista Brasileira de Geociências*, 30: 7-11.
- Van Westrenen, W., 1997. Magma mingling and mixing: the example of the Aracê/Pedra Azul magmatic complex, Espírito Santo, Brazil. MSc dissertation (unpub.), University of Utrecht, 111 pp.
- Vieira, V.S. (Ed.), 1993. *Programa Levantamentos Geológicos Básicos do Brasil*. Baixo Guandu. Folha SE. 24-Y-C-V. DNPM/CPRM, Brasília. 175 pp.
- Vieira, V.S. (Ed.), 1997. *Programa Levantamentos Geológicos Básicos do Brasil*. Cachoeiro do Itapemirim. Folha SF. 24-V-A. DNPM/CPRM, Brasília. 99 pp.

Weinberg, R.F., Sial, A.N. and Mariano, G., 2004. Close spatial relationship between

plutons and shear zones. *Geology*, 32: 377-380.

Wiedemann, C., 1993. The evolution of the early Paleozoic, late to post-collisional magmatic arc of the Coastal Mobile Belt, in the State of Espírito Santo, eastern Brazil. *Anais da Academia Brasileira de Ciências*, 65: 163-181.

Wiedemann, C.M., Bayer, P., Horn, H., Lammerer, B., Ludka, I.P., Schmidt-Thomé, R. and Weber-Diefenbach, K., 1986. Maciços intrusivos do sul do Espírito Santo e seu contexto regional. *Revista Brasileira de Geociências*, 16: 24-37.

Wiedemann, C.M., Mendes, J.C. and Ludka, I.P., 1995. Contamination of mantle magmas by crustal contributions - evidence from the Brasiliano Mobile Belt in the State of Espírito Santo, Brazil. *Anais da Academia Brasileira de Ciências*, 67: 279-292.

Wiedemann, C., Mendes, J.C., Moura, J.C., Costa Nascimento, R.C. and Ludka, I.P., 1997. Granitoids of the Espírito Santo Magmatic Arc. In: *International Symposium on Granites and Associated Mineralizations, 2, ISGAM, Salvador, Excursions Guide*, pp. 57-76.

Wiedemann, C., Medeiros, S.R., Ludka, I.P., Mendes, J.C., Moura, J.C. and Costa Nascimento, R.C., 2002. Architecture of late orogenic plutons in the Araçuaí-Ribeira Fold Belt, Southeast Brazil. *Gondwana Research*, 5: 381-399.

## A. Field Trip

In this appendix we describe key Outcrops in the region and provide enough information, so that this article can be used as a field guide:

- Day 1 - Outcrops 1 to 5;
- Day 2 - Outcrops 6 to 9;
- Day 3 - Outcrops 10 to 14;
- Day 4 - Outcrops 15 to 22;
- Day 5 - Outcrops 23 to 28.

All Outcrops described here are illustrated in Figure 30 and 31 and are close to country roads which are depicted in topographic map sheets at the scale of 1: 50 000, published by IBGE and available from the following web page: <http://mapas.ibge.gov.br>.

**Figure 30. Location map of selected Outcrops for the field trip along the coast**

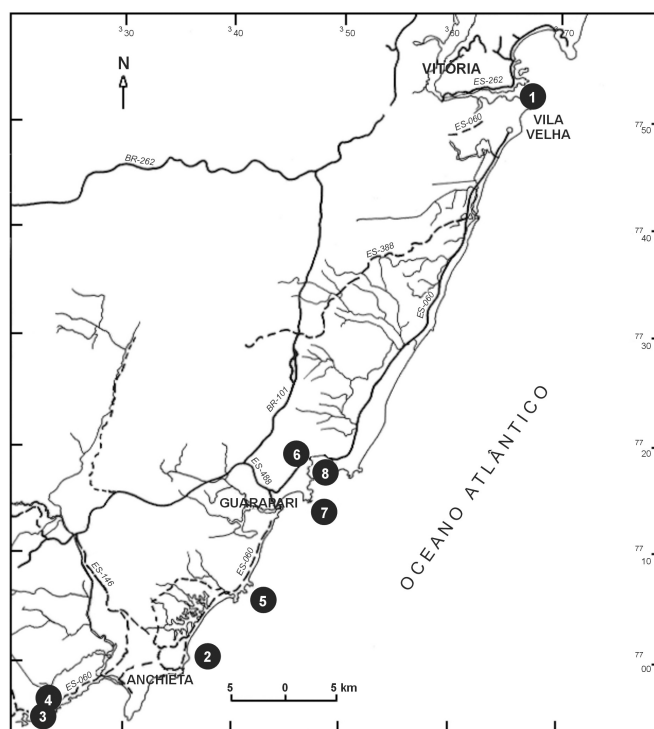


Fig. 30

Location map of selected Outcrops for the field trip along the coast.

**Figure 31. Location map of selected Outcrops for the field trip across the plutons**

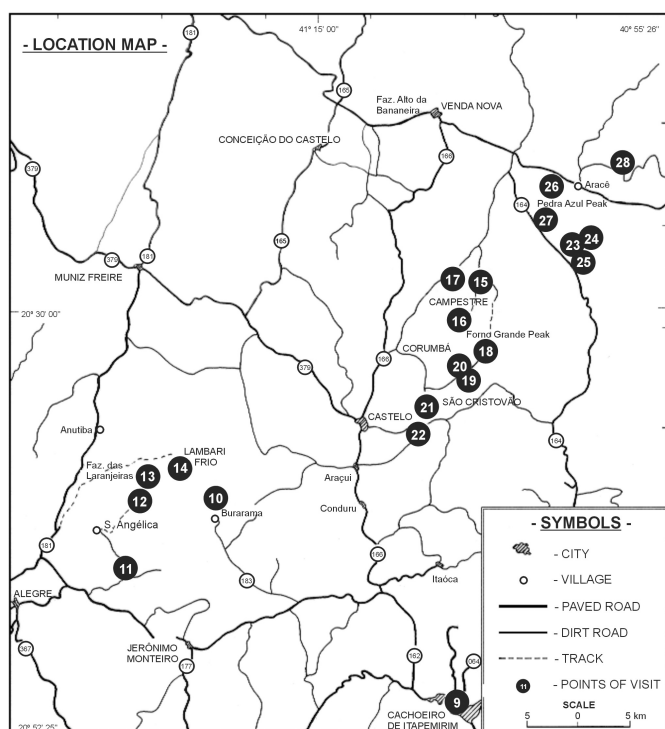


Fig. 31

Location map of selected Outcrops for the field trip across the plutons.

**The coast near Vitória and Guarapari (Costeiro complex – Figures 4 and 30)**

The main purpose of the field trip guide, along the Costeiro Complex:

1. partial dehydration melting of supracrustal Ubu-series and associated granitic products;
2. migmatic areas of magma collection, where hydrous melting and enderbitization processes compete with each other.

**Outcrop 1: Praia da Costa, in Vitória (UTM coordinates: 36630 – 775100)**

The Vitória Pluton is the easternmost intrusive body cropping out in this region. This is a multi-stage intrusion of magma under different H<sub>2</sub>O/CO<sub>2</sub>-fluid conditions and different stress regimes. In the border zone, an older greenish charnockite, with thick layers of quartz-diorite, is intruded by a pink granite. The intrusive relations can be observed along Outcrops, on the seaside of Vila Velha, Praia da Costa. In the charnockite, clear magmatic features,

such as microgranular and micaceous enclave swarms showing different degrees of deformation. Dykes of fine-grained pink granite and pegmatite veins cut the whole sequence.

**Outcrop 2: Ubu Beach in Anchieta (UTM coordinates: 33550 – 769900)**

This region is particularly interesting to observe the dehydration process in the metasedimentary pile. The beach of Ubu, the type locality for the Ubu-series (Paraíba do Sul Complex), is located approximately 15 km north of Iriri city. Here a sequence of migmatitic cordierite-sillimanite-garnet-biotite gneisses (kinzigite) crop out. Several folded and partially boudinaged calc-silicate layers, point towards a heterogeneous, primary sedimentary rock package. At least two migmatization phases can be recognized: a) folded ptigmatic, and b) unfolded leucosomes. The latter is preferentially emplaced along ductile shear zones, where garnet-rich granitic melt intrudes ( Figure 8 ).

**Outcrop 3: Pau Grande Beach in Anchieta (UTM coordinates: 32500 – 769630)**

In this region, the G2 hypersthene-bearing enderbites (tonalite, granodiorite, granite) crops out. This rock is comprised of oligoclase, K-feldspar, quartz, biotite, garnet, hornblende and hypersthene. Common accessory minerals are apatite, zircon and ore minerals. Calc-silicate layers, similar to those observed in the Ubu series, is a strong field argument supporting the origin of this sequence through dehydration melting of the Ubu series such as in Outcrop 2.

**Outcrop 4: Small quarry close to Iriri town (UTM coordinates: 332850 – 7769700)**

In this quarry a migmatized garnet-biotite gneiss probably part of the Ubu series (Paraíba do Sul Complex) depicts irregular patches of greenish color related to the incomplete formation of enderbite. The metamorphic rocks are intruded by granite and pegmatite veins, from the latest production of granitic melts.

**Outcrop 5: Outcrops on the Enseada Azul Beach (UTM coordinates: 34150 – 770680)**

This is an interesting point to observe the development of augen gneiss textures. A garnet-rich gneiss sequence with similar textures to that of the Ubu series (Paraíba do Sul Complex) as in Outcrop 2, but more intensely migmatized, crops out in this point. Thick bands showing feldspar

augen are interlayered throughout the sequence. There are larger amounts of garnet-rich G3 granitoids, originated from the partial melting of the gneisses, but this locally formed granitoid is not seen to form large, independent granitic bodies. Some relicts of refractory melanosome are preserved.

### ***The Guarapari coast and the cachoeiro de itapemirim region (Figs 4, 5 and 6)***

#### ***Outcrop 6: Quarry north of Guarapari (UTM coordinates: 34750 – 771930)***

Quarry with evidence regarding the origin of enderbites through alteration/metasomatism of the gray metaigneous gneisses. Here a homogeneous tonalite to granodiorite (probably G1) has been partially remolten to generate leucocratic veins. Several irregular domains of enderbite in a metatonalitic to metagranodioritic rock can be observed on a much larger scale. The gneiss carries some poikilitic microcline porphyroblasts, in an oligoclase-quartz-biotite-matrix of tonalitic composition. In the green domains of the metatonalite, where the rock is changed into an enderbite, relicts of metamorphic clinopyroxene are usually found. A later phase of retrometamorphism caused the replacement of clinopyroxene by hornblende and biotite, illustrating the change of H<sub>2</sub>O/CO<sub>2</sub> fluid conditions during metamorphism.

#### ***Outcrop 7: Ponta do Pescador Outcrop (UTM coordinates: 34700 – 771500)***

In this Outcrop there is:

- a. the gradational evolution of kinzigite towards augen gneissic layers of granodioritic and granitic composition;
- b. in situ dehydration melting of the metasedimentary pile. A package of sillimanite-cordierite-garnet-biotite gneiss (kinzigite of the Ubu series, Paraíba do Sul Complex similar to outcrop 2) has undergone partial dehydration melting to form more homogeneous tonalitic to granodioritic layers ascribed to G2. The northern part of the Outcrop contains calc-silicatic layers and lenses (Ubu series) and records amphibolite facies conditions. In the southern part of the Outcrop, the general texture of the rocks changes gradually into an igneous texture and a more homogeneous hypersthene-rich and garnet-poor enderbite

suite crops out. Large microcline porphyroblasts are common and account for more K-rich compositions.

Local ductile shear zones with granitic neosome cut the package. The last magmatic event in this area is related to the intrusion of post-kinematic fine- to medium-grained granites and pegmatite veins.

#### ***Outcrop 8: Perocão Beach (UTM coordinates: 34903 – 771750)***

An homogeneous granitoid gneiss can be observed along the stairs to the Perocão beach. This Outcrop depicts, in a small scale, the complexity of the geology in the area (fig. 6). The dominant lithology is a G2 suite metagranitoid (augen amphibolitic gneiss from the Costeiro Complex) with G2 enderbitic portions. Two augen-gneiss types were described in the area: 1) a zircon-cordierite-garnet-biotite-quartz-plagioclase (An<sub>23-25</sub>), and 2) an apatite-zircon-amphibole-plagioclase (An<sub>28-43</sub>) gneiss. Both grade into hypersthene-bearing enderbitic rocks (Teixeira, 1998). A retrometamorphic event is depicted by the replacement of hypersthene by biotite and amphibole. The gneiss package is locally interlayered with leucogneiss (biotite-poor-garnet-quartz-microcline-plagioclase gneiss or leptinite) and biotite-garnet-quartz-microcline-plagioclase gneiss. Gneisses in this Outcrop are partially molten giving rise to migmatites. Walking along the Outcrop, local K-feldspar augen gneiss grades into quartz-feldspar-garnet gneiss layers, so that augen-gneiss bands alternate with leptinites. The predominant gneissic foliation is E-W / NE-SW (Fig. 6). Ductile N-S shear zones are the usual paths for these intrusions. G2 enderbitic gneisses are interlayered with amphibolitic gneiss, in a similar situation (as in Fig. 5). Along the ductile shear zones, probably due to local H<sub>2</sub>O-rich fluids, a retrometamorphism process may be observed in the granulitic rocks. Younger tonalitic/granodioritic dykes and sills, containing granitic and/or pegmatic schlieren, intrude the Outcrop and are considered to be related to the bimodal post-collisional magmatism (G5). This region seems to be a magma-collecting zone for the late intrusion of G5 granitoids. This is clearly depicted on the detailed map on Fig. 6. N-S trending younger intrusions in the amphibole/biotite gneisses are pegmatite richer, while granodiorite/tonalite batches concentrate closer to the green hypersthene-rich patches (enderbitic suite).

#### **Outcrop 9: (UTM coordinates: 27540 – 769500)**

In the city of Cachoeiro de Itapemirim, one of Brazil's leading natural stone factories should be visited. Visitors are generally welcome at Braminex and GranBrasil factories. The several rocks from the region can be enjoyed as polished slabs.

### **G5 complex zoned plutons - magma mixing and mingling in a deep plutonic environment**

#### **Santa Angelica - A frozen-in magma mixing - Outcrops 10 - 14 (Figures 15 and 31)**

The Outcrops of this pluton, described below, include examples of the country rock surrounding the complex, intrusion mechanism, shearing of plutonic rocks as well as different mingling processes and textures.

#### **Outcrop 10: Floresta valley, approximately 3 km northward of Burarama (UTM coordinates: 25506 – 771208)**

Northwest and west of the Santa Angélica Intrusive Complex (SAIC), a granodioritic gneiss (Estrela Batholith, G1 suite) crops out, extending northwards until the Guaçu Lineament (Fig. 2). This rock-type has a coarse-grained homogeneous augen texture with an amphibolite-facies metamorphic foliation (D1) (Bayer, et al., 1986). In the contact zone with the SAIC (G5 suite), this D1 foliation was deformed plastically together with microdioritic dikes from the intrusion (Bayer, 1987; Wiedemann et al., 1997).

#### **Outcrop 11: Selva de Pedra Quarry (UTM coordinates: 24604 – 770507)**

At the southeastern border of the SAIC, the internal marginal zone is made up of an almost continuous ring of coarse-grained granite (Granite I, analysis SA4.1, Table 1), showing strong magmatic flow-structure parallel to the border (Wiedemann et al., 1997). In this Outcrop, the earlier flow-structure of the granite is gently undulated and overprinted by a second ductile foliation. The quarry is at the very contact between the gneiss and granite I. Blocks showing this contact can be seen. Sills of the granite intrude the enclosing gneiss *lit par lit* (Fig. 18). The contacts are sharp but irregular and produce an injection migmatite. The schistosity of the gneiss is chaotically folded and partially melted, with clear separation of leucosome and melanosome. Strongly deformed basic enclaves can be observed in the granite.

#### **Outcrop 12: Bela Aurora Quarry and surroundings (UTM coordinates: 24500 – 771100)**

This is a region of homogeneous gabbro-norites and gabbro-diorites. In the homogeneous dark matrix, K-feldspar xenocrysts may be found as drops together with granitic schlieren.

The composition of clinopyroxene in the gabbros shows small variations in the fields of salite and augite. Orthopyroxene is mostly hypersthene (Schmidt-Thomé, 1987). A single analysis of pigeonitic composition is probably due to several submicroscopic exsolution lamellae of cpx in opx. Exsolution of ilmenite is also common in pyroxene. Secondary amphibole after pyroxenes are mostly edenitic hornblende with higher Si- and Mg-contents than the quartz poikilitic magnesium hastingsitic hornblende from the megacrysts and matrix. The TiO<sub>2</sub>-content of biotite reaches levels up to 3.56% and MgO up to 13.82% (Schmidt-Thomé, 1987). A characteristic microfabric of these gabbros is the coalescence of plagioclase crystals in synneusis (Wiedemann, et al., 1986). This could be a sign for an abrupt lowering of crystallization temperature which stopped further magma mixing. Apatite, as fine acicular needles, is a common accessory mineral. No olivine has been found. See Table 1, SA2.1 for chemical analysis.

#### **Outcrop 13: Pireneus Ridge (UTM coordinates: 24608 – 771502)**

In this region, mingling of magmas, from microscopic to metric scales, is exposed (Fig. 20). Different corrosion stages of feldspars, differently mantled feldspar and quartz xenocrysts are noteworthy (Fig. 21). Granitic schlieren mingle with the basic magma producing a pillow network. Local mixing originates intermediate rocks of granodioritic composition (Table 2, chemical analyses: SA 2.1; SA2.2; SA 3.1; SA 3.2; SA 3.3).

#### **Outcrop 14: Lambari Frio (UTM coordinates: 25400 – 771503)**

This is a hybrid zone, similar to that of the Pireneus Ridge. Here, strong deformation, probably due to a shear zone, caused more intense mixing of different lithologies resulting in rocks that look like a banded gneiss (Fig. 22).

#### **Castelo Complex - A frozen-in contact - Outcrops 15 to 22 (Figure 23)**

Seven Outcrops of the Castelo Complex are described below. They reveal the nature of this inversely zoned, mingled pluton and the nature of its contacts with country rock

gneisses. In this complex, a porphyritic, fine-grained sphene monzogranite (granite II), very similar to the granite II of Santa Angélica, crops out in the border region, in contact with the enclosing gneisses. It forms most of the matrix of a thick agmatic border. It consists of rafts of the enclosing gneisses in a granite-II matrix and suggests stopping. This granite II may also intrude the border gneisses as *lit par lit* sills or discordantly, as dykes along shear zones (Fig. 24).

**Outcrop 15: (UTM coordinates: 28050 – 773400)**

From the BR-262 take the asphalt road Venda-Nova-Cachoeiro do Itapemirim, shortly after the small village of São Paulino (on the topographic IGBE map) take the country road to Alto Santa Clara.

A coarse-grained granodiorite is intruded by several dikes of a porphyritic granite giving rise to net-veined structure. The megacrysts consist of K-feldspars. Gradation between granite and granodiorite may also be observed.

**Outcrop 16: Córrego Santa Clara (UTM coordinates: 28020 – 773303)**

This is the core of the intrusion, dominated by coarse-grained diorite. Shrinkage cracks (Hibbard and Watters, 1985) formed during solidification are intruded by granite. Walking along the river, there are local changes in the diorite grain size, tending to a finer texture due to the contact with coarse-grained granite. The contact is characterized by a frozen layer of mingled microdiorite and granitic schlieren (Fig. 25).

**Outcrop 17: Alto do Caxixe Quente - 1 km away from the Santa Clara Church (UTM coordinates: 27909 – 773402)**

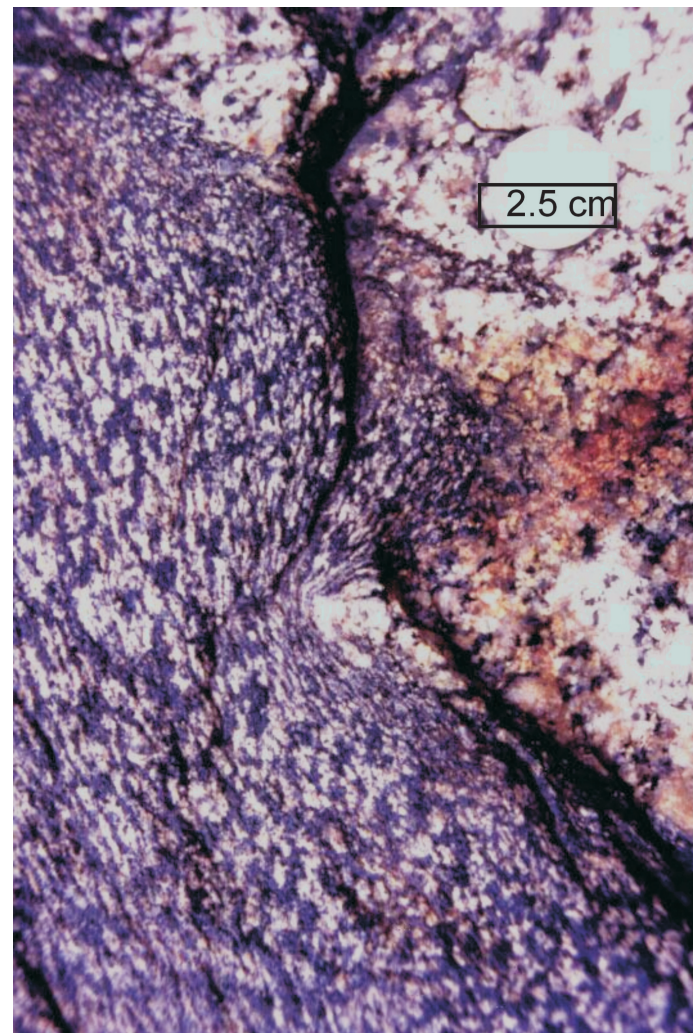
A very interesting Outcrop of Granites I and II in close proximity showing:

1. magmatic banding of granite I and II with foliation parallel to the margins of the intrusion;
2. feldspar megacryst imbrication and deformation due to viscous magmatic flow;
3. discordant contact between a syn-intrusive microdioritic dike showing strong magmatic foliation and a coarse-grained granite I ( Figure 32 ). This is a hybrid monzodiorite with a glomeroporphyritic texture, with hornblende + biotite + apatite + ilmenite + magnetite clots surrounded by a titanite rim. Poikilitic

hornblende contains biotite, opaque minerals, acicular apatite and sphene. Strongly zoned plagioclase grains are randomly dispersed in the very fine-grained diorite matrix;

4. zone of different layers of the two granites (I and II) in sub-parallel contact with less evolved elongated magma blobs (pillow-like structure) of diorite to granodiorite, in different degrees of mixing with the granites. Presence of xenocrysts of corroded quartz and mantled feldspars in the mafic pillows. Under the microscope, common acicular apatite indicates rapid cooling during crystallization.

**Figure 32. Castelo Complex**



Discordant contact between a synintrusive microdioritic dike, showing strong flow deformation at the border, and coarse-grained granite.

The most usual minerals are: andesine, augite, hornblende, sphene, apatite and zircon. Occasionally, quartz

content increases, mostly as corroded xenocrysts surrounded by mafic minerals and the rock becomes a quartz diorite. K-feldspar is rare; augite may be replaced by hornblende or by biotite, accompanied by exsolution of ilmenite and Ti-magnetite, parallel to the 001 cleavage of the augite. Less frequently the diorite may contain small amounts of subhedral opx.

**Outcrop 18: The hybrid zone at Forno Grande (UTM coordinates: 28200 – 773000)**

Most of the magma-mingling features seen in Santa Angélica are also present in Castelo. However, here granite mingles with dioritic and granodioritic magmas, showing similar quartz xenocrysts with mafic aureoles and mantled feldspars, like those from Santa Angélica. Coarse-grained granite forms a net-veined structure with the microdiorite. At the bottom of a small waterfall, spotted fine-grained granite, rich in surmicaceous enclaves, which are aligned parallel to the magmatic flow, crops out. Going up hill, differently shaped enclaves are embedded in a porphyritic granite (type-II). Pillow-like structures of different types can be observed:

1. fine-grained microdioritic;
2. medium grained dioritic showing different hybridization degree with the granite;
3. local more homogeneous hybridization between granite and diorite originating granodioritic portions;
4. spotted textures (Hibbard, 1995) and granitic schlieren in the microdiorite;

**Outcrop 19: Fine-grained sphene granite of São Cristóvão (UTM coordinates: 27808 – 772401)**

A fine-grained granite, similar to the Santa Angélica granite II, typically Outcrops close to the contact of the pluton with the country rock. This same granite also forms layers in the coarse-grained granite I, towards the center of the structure. The foliation is always parallel to the pluton margin. This granite is occasionally porphyritic with microcline megacrysts in a monzogranitic matrix. The accessory minerals are titanite, zircon, apatite, magnetite, ilmenite, pyrite, chalcopyrite and allanite. Gradational contacts between diatexitic rocks, from the enclosing gneisses, and this granite are common. Ghost structures from the gneisses are possible evidence for the anatectic origin of this granite. Surmicaceous enclaves parallel to magmatic foliation are also common.

**Outcrop 20: Megaporphyritic granite (Granite I). Quarry in São Cristóvão (UTM coordinates: 27805 – 772406)**

Close to Outcrop 19, very homogeneous coarse-grained granite, with well-developed magmatic flow given by K-feldspars megacrysts, crops out. Enclaves with intermediate to basic compositions are stretched and deformed, parallel to the main flow direction. Sphene is the most common accessory mineral.

**Outcrop 21: Boulder (blasted open) of a fine-grained diorite with irregular granitic schlieren (UTM coordinates: 27600 – 772203)**

Spotted textures are a common feature for mafic rocks of the Castelo Complex. This texture is formed by a glomeroporphyritic aggregate of mafic minerals (pyroxenes and/or amphibole and biotite clots) in a microdioritic matrix. Xenocrysts of quartz surrounded by a mafic aureole are often present in this unit. Biotite concentrations may be observed at the contact between the granitic schlieren and the microdiorite. Analyses of similar rocks in Table 1: Ca 1.1 and Ca 1.2.

**Outcrop 22: Migmatite border zone of the Castelo Complex (UTM coordinates: 27600 – 772106)**

A migmatitic zone borders most complex plutons of this belt. In this Outcrop, the D1-foliation of the gneiss is chaotically refolded.

**Pedra Azul - Mature Magmatism - Outcrops 23 - 28 (Figure 23)**

The Pedra Azul Complex crops out in the center-southern region of Espírito Santo. This inversely zoned pluton is formed by contrasting lithofacies grading from quartz diorite to syenogranite (Costa Nascimento et al., 1996; Fig. 23). Inside the pluton, a medium-grained monzogranite forms the highest peaks as well as the lower border regions, forming the magmatic envelope of the structure. Several portions of tonalite to granodioritic compositions were mapped towards the center of the structure. Evidence for magma mingling processes are sharp contacts between coarse- and fine-grained contrasting lithotypes, acicular apatite grains in mafic pillows, mantled and corroded feldspars, corroded / embayed biotite and other mineral instability textures.

**Outcrop 23: Border region of the pluton (UTM coordinates: 28903 – 774602)**

A fine- to medium-grained paragneiss megaxenolith can be observed in the monzogranite. At the contact between the xenolith and the granite, partial melting is evidenced by intrusive lit-par-lit interfingering. The local partial melting of the xenolith also produced aplitic veins that intrude the granite.

**Outcrop 24: Mixed zone in the southern portion of the pluton (UTM coordinates: 28905 – 773900)**

A layered structure, formed by stretched pillow-like tonalitic/granodioritic enclaves ( Figure 33 ) can be followed over one hundred meters. Felsic coarse-grained granitic schlieren and veins surround and/or intrude the enclaves.

**Figure 33. Tonalitic/granodioritic enclaves**



Layered structure formed by stretched pillow-like tonalitic/granodioritic enclaves or layers and medium-grained granite. Pedra Azul Pluton.

**Outcrop 25: Magmatic flow (UTM coordinates: 28903 – 773806)**

Coarse-grained monzogranite, showing large feldspar crystals aligned along a NW-SE magmatic flow trend.

**Outcrop 26: Mixed zone in the NW portion of the pluton (Pousada Pedra Azul Hotel) (UTM coordinates: 28800 – 774400)**

Mixed zone characterized by a net-veined/pillow-like structure. Tonalitic/granodioritic pillow-like and angular enclaves are chaotically distributed and wrapped by felsic medium- grained monzogranitic veins. Pegmatite veins is the last intrusive event.

**Outcrop 27: Enclave swarm in a mingled zone (UTM coordinates: 28740 – 774205)**

This Outcrop is characterized by several types of aulitic and xenolithic enclaves, showing variable shapes and dimensions, and different assimilation degrees. The matrix is a medium- to coarse- grained rock. Some enclaves have clear reaction borders, grading from diffuse to sharp contacts. A very interesting feature is the presence of bimodal enclaves diorite/granodiorite, probably formed during the mingling process. The irregular distribution of the enclaves points toward a local turbulent magmatic flow.

**Outcrop 28: The ocellar texture of the syenogranite (UTM coordinates: 29003 – 774602)**

In this stop, an exotic ocellar texture can be observed in the fine-grained syenogranite. This rock consists of rounded leucocratic ocelli, wrapped by a mesocratic biotitic rim. The ocelli are essentially sphene-centered aggregates of microcline and quartz, with minor amounts of allanite. Microcline, quartz, biotite, plagioclase and accessory phases (zircon, allanite, opaque minerals and fluorite) form the matrix.



**Table 3. Chemical analyses of intermediate and acid rocks (g5- monzosienites, granodiorites to granites)**

S a m p l e	C A 3 1	C A 3 2	V N 1	V N 2	V N 3	S A 4 1	S A 4 2	C A 4 1	C A 4 3	C A 4 4	V N 4 1	V N 4 2	V N 4 3	S A 5 2	S A 5 3	S A 5 4	C A 5 1	C A 5 2	C A 5 3	
<b>S i O 2</b>	61.89	66.57	58.95	59.07	66.74	77.81	68.21	77.48	77.40	77.40	77.46	77.41	77.43	66.62	66.80	67.42	77.75	77.91	77.92	77.74
<b>T i O 2</b>	1.74	0.74	0.93	1.00	0.84	0.41	0.85	0.35	0.55	0.35	0.52	0.81	0.77	0.00	0.00	0.00	0.66	0.66	0.76	0.41
<b>A l 2 O 3</b>	14.86	15.82	26.08	26.02	19.75	11.84	12.43	14.37	13.50	16.07	11.77	11.99	11.92	14.82	14.74	14.24	11.47	14.04	14.11	13.85
<b>F e O</b>	5.76	3.68	2.36	2.01	3.83	1.61	2.19	1.64	1.85	0.03	0.08	0.06	0.05	4.19	2.96	2.00	2.29	2.02	2.91	1.55
<b>F e O 3</b>	1.02	0.65	1.57	1.16	2.81	0.47	0.66	0.27	0.27	0.00	0.05	0.05	0.03	0.00	0.00	0.00	0.67	0.71	0.14	0.42
<b>M g O</b>	2.66	1.49	0.55	1.30	1.66	0.39	0.85	0.22	0.52	0.00	0.00	0.00	0.00	0.00	0.00	0.00	0.00	0.00	0.00	0.00
<b>C a O</b>	4.00	2.44	2.09	3.19	5.38	1.60	2.75	1.59	1.42	1.10	0.25	0.33	0.48	4.29	2.37	1.89	1.14	1.44	1.46	1.19
<b>N a O</b>	1.29	2.18	1.99	3.99	3.40	3.33	2.38	2.84	2.16	1.21	1.64	1.48	1.89	2.20	2.03	2.03	2.24	2.39	2.99	1.30
<b>K 2 O</b>	0.39	4.85	6.38	6.88	1.47	3.38	5.38	6.20	5.92	6.52	5.94	5.52	5.94	1.59	5.94	4.98	5.42	5.94	5.98	4.33
<b>M n O</b>	0.00	0.00	0.00	0.00	0.00	0.00	0.01	0.00	0.00	0.00	0.00	0.00	0.00	0.00	0.00	0.00	0.00	0.00	0.00	0.00

